Modelling and analysis of a hybrid solar concentrating-waste incineration power plant

Sadi, Meisam; Arabkoohsar, Ahmad

Published in:
Journal of Cleaner Production

DOI (link to publication from Publisher):
10.1016/j.jclepro.2018.12.055

Publication date:
2019

Document Version
Accepted author manuscript, peer reviewed version

Accepted Manuscript

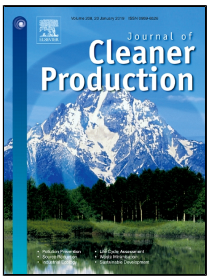

Modelling and Analysis of a Hybrid Solar Concentrating-Waste Incineration Power Plant

M. Sadi, A. Arabkoohsar

PII:	S0959-6526(18)33757-0
DOI:	10.1016/j.jclepro.2018.12.055
Reference:	JCLP 15113
To appear in:	*Journal of Cleaner Production*
Received Date:	08 August 2018
Accepted Date:	05 December 2018

Please cite this article as: M. Sadi, A. Arabkoohsar, Modelling and Analysis of a Hybrid Solar Concentrating-Waste Incineration Power Plant, *Journal of Cleaner Production* (2018), doi: 10.1016/j.jclepro.2018.12.055

Modelling and Analysis of a Hybrid Solar Concentrating-Waste Incineration Power Plant

M. Sadi[1], A. Arabkoohsar[2,*]

[1]Department of Mechanical Engineering, Islamic Azad University, Shahrood Branch, Shahrood, Iran

[2]Department of Energy Technology, Aalborg University, Denmark

*Corresponding author: ahm@et.aau.dk

Abstract

Concentrating solar power plant will be a key component of the future energy systems in which the share of renewable energy is extremely high. A major challenge of this technology is, however, its intermittent power output, slowing down its rate of implementation in the global energy matrix. As such, waste incineration is a popular technology in the developed countries as a smart measure for the disposal of municipal waste and generating free energy. In this study, a hybrid configuration of a concentrating solar power plant accompanied with a waste incineration unit is proposed. In the proposed system, the waste incinerator offers a variable heating duty in order to regulate the power output of the concentrating solar power plant. The hybrid plant is designed for a case study in Denmark and is thermodynamically analyzed. The results of the simulations are presented and discussed. It is shown that the hybrid system can pave the bed for increasing the share of solar thermal power and bringing more waste incinerators to the electricity market. A 10 MWe hybrid power plant may prevent up to 8,000 tonnes of carbon dioxide equivalent emission per month. The overall efficiency of the hybrid system is expected to be 24%.

Keywords: Concentrating solar power plant; Waste incineration; Intermittent power output; Greenhouse gas emission; Thermodynamic analysis.

1. Introduction

Improving energy efficiency and reducing both energy demand and greenhouse gas emissions are major challenges for today's energy systems. For these, while there is no straightforward solution, research and development in thermal energy management has continuously striving to find sustainable measures [1]. One of the main features of the future energy system is the high share of renewable energy, while the strong synergy between the energy system components and energy sectors will be another vital characteristic of that [2].

Among the known renewable energy technologies, solar energy has emerged as a viable, cost- effective and commercial option for grid connected power generation [3]. Among solar power technologies, today, photovoltaic (PV) is more of interest than concentrating solar power (CSP) due to its less capital investment, simpler technology, and better economic performance [4]. The CSP technology, however, will also be an important and active part of the future energy systems. This is due to the inertia service that such power plants provide for the grid, whereas a PV farm is unable to provide this service for grid frequency stabilization [5]. There are a large number of studies in the literature assessing the further development of CSP plants all over the world. Smith [6] evaluated the long-term market potential of CSP systems in a global scenario. He examined the conditions under which CSP systems might play a larger role in the global energy system during the twenty-first century. Belgasim et al. [7] evaluated the potential of CSP for electricity generation in Libya by reviewing the energy sector and socio-economic context of the country, assessing site parameters and meteorological data as well as accomplishing the required techno-economic simulations. Balghouthi et al. [8] presented a thorough analysis of the suitable factors for the deployment of CSP technology in Tunisia. They also discussed the possibility of electrical interconnection between Tunisia and Italy, and evaluated the opportunity of the exploitation of renewable energy technologies such as CSP plants in North Africa by European countries. Ogunmudimu and Okoroigwe [9] presented a review of CSP installations in Nigeria, and analyzed the possibility of further implementation of such power plants in this country. They proposed parabolic trough technology for immediate establishment due to the technology development, investment, land and water requirements in the country, and solar tower technology for middle and long-term projects.

A major challenge of a CSP plant is the intermittency of the source of energy, making the power output of the plant unreliable and fluctuating. The literature presents a large number of studies proposing solutions for overcoming this challenge. Overall, one of the main solutions to this problem of renewable energy plants is employing energy storage technologies to manage the power output of the plant be stable and dispatchable [10]. For a CSP plant, both thermal and electrical storage technologies are the possibilities. Mao [11] presents a thorough review of the most recent developments in geometrical configurations of thermal

energy storage for CSP plants. Prieto et al. [12] present a review of thermochemical energy storage for CSP plants. The other solution is a hybridization of a CSP plant with a secondary source of heat or power. McTigue et al. [13] proposed the hybridization of a geothermal power plant with a CSP plant accompanied with a thermal storage in order to increase the power output and dispatchability of the plant. This configuration resulted in an enhancement of the electricity conversion efficiency for 24% and a reduced capital investment of 15% for the same power capacity. Cavallaro et al. [14] represented a review of hybrid CSP plants with various natural gas technologies and ranked the solutions based on an intuitionistic fuzzy multi-criteria algorithm. Jin and Hong [15] reviewed the potential of hybrid CSP-fossil fuel-based power plants and outlined the various arrangements and methods. Behar [16] presented a detailed review and thermal performance comparison of various hybrid solar systems (including CSP) with other technologies. In this work, various integrations of solar parabolic trough technology into the three power conversion cycles of Brayton, Rankine and combined power were considered. Manente et al. [17] analyzed a selected number of integrated solar (including parabolic trough, linear Fresnel and solar tower) combined cycle layouts. They concluded that in the best layout, solar heat is used for the evaporation of high-pressure saturated water and through an exergy analysis, they explained why some layouts make a better use of solar energy.

On the other hand, although some NGOs (non-governmental organizations) are against waste incineration (WI) because they believe it is not guaranteed to not emit hazardous emissions in the future, others look at it as a sustainable method of energy production and a highly beneficial technology for the production of free heat or electricity. According to the European Waste Incineration Directive [18], the flue gas temperature of a WI unit should reach at least 850 °C to ensure the proper breakdown of toxic substances. In addition, the alternative method to incineration is landfilling, which requires a large space and results in the emission of hazardous pollutants [19]. Today, WI is a popular technology for heat and power production in a number of European countries, such as Denmark, Germany and the Netherlands [20]. There is a variety of urban, industrial and service applications of WI technology. Ghouleh and Shao [21] assessed the potential for redefining WI into a cleaner cement production, where locally-sourced heat, ash, and emitted CO_2 can be used to generate products for building applications. Munster and Meibom [22] presented a study aiming at the optimization of the use of waste in the future energy system. The analyzed system includes both the heat and the electricity markets. Erikson et al. [23] assessed the performance of WI units, based on two schemes of heat only production and heat and power production, in the district heating system of Denmark. They also compared the obtained results with district heating systems supplied by other technologies such as biomass and natural gas plants. National Aeronautics and Space Administration accomplished a project of hybrid pyrolysis/incineration system for solid waste resource recovery. This integration took advantage of the best features of each process and resulted in an overall reduction of system complexity [24]. Udono

and Sitte [25] presented a modeling of waste heat powered plant for seawater using a dynamic system approach. The modeling approach was complemented with other modeling techniques such as artificial neural networks to overcome a number of modeling difficulties. Hedberg and Danielssen [26] presented a thorough feasibility report of WI powered absorption chillers for cold production in Thailand, found as an interesting proposal.

Taking into account the presented facts about the CSP and WI technologies, and considering the critical role of WI systems in the European (and probably global in the near future) energy matrix, this study proposes the utilization of a WI unit for the stabilization of the power output of CSP plant. For this, a hybrid configuration is proposed. In this hybrid system the WI system provides auxiliary heat for the hot/vaporized working fluid coming from the parabolic trough collectors (PTCs) to reach the desired temperature before the expansion. Thus, the WI unit provides a variable heating duty for the hybrid system in which the load depends on the availability of solar irradiation. By such an integration, the proposed hybrid system offers several valuable advantages for the electricity grid, such as increased dispatchability and reliability, improved efficiency, reduced capital costs through equipment sharing, and the opportunity for flexible operation by alternating between energy sources. The system is designed and analyzed for a case study in Denmark, where there are several WI plants and constructing solar power plants in the future is a planned policy. The developed system is simulated pseudo-dynamically over an entire year of operation and the results are presented and discussed.

Note that the main novelty of this work is about its innovative hybrid solar-waste configuration proposed for the first time. It is well known that it might be highly beneficial to have a supplementary power/heat production unit along with the fluctuating renewable based systems, e.g. solar and wind technologies. In this way, the energy output of the system will be better dispatchable and efficiently tradeable in the electricity market. As such, another contribution of this work is introducing a smart way of solving the waste management problem in the societies. Since WI is a key component of smart energy systems, therefore, there should be more efficient and smarter ways of employing WI units, rather than being simply a standalone energy system. In the proposed system, not only the WI unit is doing its main function, i.e. power production, but also it is supporting the fluctuating power output of a solar system to be reliably supplied to the grid.

2. The Hybrid System and the Modeling Method

In this section, the configurations and the technical characteristics of the proposed integrated power plant are explained and the mathematical models are presented.

2.1. System layout

As explained, the proposed combined system is a CSP plant hybridized with a WI unit. In fact, it is an integrated PTC and WI (IPTC-WI) power plant, which is a Rankine cycle using solar energy and municipal solid waste energy as its heat input. Figure 1 illustrates the configuration of the Rankine cycle based IPTC-WI power plant. According to the figure, the system is based on a regular steam power plant with three high-, medium- and low-pressure turbine stages. The cycle has a regeneration loop just before the medium-pressure turbine. In addition, there are two preheating lines of the feed-water with a portion of the steam from the regeneration line and at the middle of the second turbine.

In this system, the primary source of heat of the plant is provided by the PTC array which is transferred to the plant working fluid via a heat exchanger (Boiler-1). Depending on the amount of solar energy available, the working fluid coming out of the collector modules may reach a specific temperature, and consequently, the power plant working fluid can reach a certain temperature through the first boiler. Then, the WI unit supplies the rest of the heat required to increase the working fluid temperature up to the desired level before the expansion process through the steam turbines. This heat is given to the power plant working fluid via a second heat exchanger (Boiler-2) which is the source of the regeneration as well.

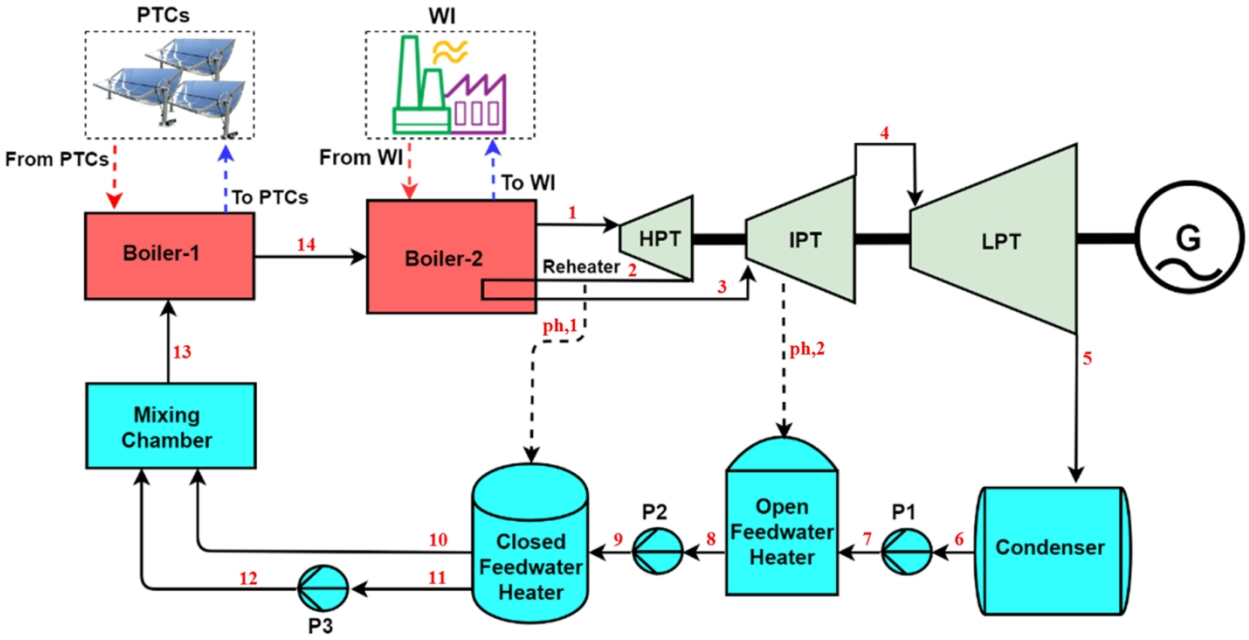

Figure 1 – A Rankine cycle based IPTC-WI plant including reheat and regeneration lines; P: pump, HPT: high-pressure turbine, IPT: medium-pressure turbine, LPT: low-pressure turbine, G: generator.

2.2. The system model

Before presenting the detailed model of the hybrid system and the components, a list of assumptions/simplifications made for simulating the performance of the system is given:

- Solar irradiation is assumed constant during each hour.
- The effect of humidity on the performance of the system components is negligible.
- Pressure losses through the installations and heat exchangers are negligible.
- Waste used in the WI unit is sufficiently mixed and presents a uniform heating value.
- The effects of the off-design operation of the system components are neglected.
- The inlet temperature and pressure of the turbines are fixed and the mass flow rate of the working fluid varies for load variation.

For starting the modeling of the system, one should know how much electricity the power plant should produce at every moment. Having this factor as $\dot{E}_{gen}$ and the electricity generator efficiency as η_{gen} (0.95), one may calculate the rate of power produced by the turbines as below:

$$\dot{W}_{net} = {\dot{E}_{gen}}/{\eta_{gen}}; \quad \text{where: } \dot{W}_{net} = \overbrace{\dot{W}_{hpt} + \dot{W}_{ipt} + \dot{W}_{lpt}}^{\dot{W}_T} - \overbrace{\Sigma \dot{W}_p}^{\dot{W}_P} \tag{1}$$

in which, $\dot{W}$ is the work production rate and the indices *hpt*, *ipt* and *lpt* stand for the high-, medium- and low-pressure turbines, respectively. $\Sigma \dot{W}_p$ refers to the summation of the work used by the pumps.

Knowing the amount of power that should be produced, the inlet and outlet temperature and pressures of the pumps and turbines, and the isentropic efficiency of the turbines and the pumps (both 0.85), one may calculate the total work of the turbines, the pumps as well as the mass flow rate of the steam flow at different points on the cycle by the following equations [27]:

$$\dot{W}_T = \dot{m}_1 w_{hpt} + \left(\overbrace{\dot{m}_2 - \dot{m}_{ph1}}^{\dot{m}_3}\right) w_{ipt,I} + \left(\overbrace{\dot{m}_3 - \dot{m}_{ph2}}^{\dot{m}_4}\right)\left(w_{ipt,II} + w_{lpt}\right) - \dot{m}_{st} \sum w_p \tag{2}$$

$$\dot{W}_P = \dot{m}_6 w_{p1} + \left(\overbrace{\dot{m}_7 + \dot{m}_{ph2}}^{\dot{m}_8}\right) w_{p2} + \left(\overbrace{\dot{m}_{ph1}}^{\dot{m}_{11}}\right) w_{p3} \tag{3}$$

where, $\dot{m}_j$ is the mass flow rate of steam at point *j* of the cycle (marked on Figure 1), w is the specific work of the turbines and pumps which is calculable by simple thermodynamic relations [28]. As such, $\dot{m}_{ph1}$ and $\dot{m}_{ph2}$ are the mass flow rate of steam through the first and second preheating lines. The subscriptions *ipt,I* and *ipt,II* refer to the first and second halves of the medium pressure turbine.

For the condenser, the heat that should be rejected from the steam flow after the low-pressure turbine to make it condensed is given by:

$$\dot{Q}_{cond} = \dot{m}_5(h_6 - h_5) \tag{4}$$

where, h_5 and h_6 are consequentially the enthalpies of the water/steam flow before and after the condenser.

For the energy balance of the closed feed water tank, the open feed water tank, and the mixing chamber the following three equations are employed.

$$\dot{m}_{ph1}h_2 + \dot{m}_9h_9 = \dot{m}_{10}h_{10} + \dot{m}_{11}h_{11} \tag{5}$$

$$\dot{m}_{ph2}h_{ph2} + \dot{m}_7h_7 = \dot{m}_8h_8 \tag{6}$$

$$\dot{m}_{10}h_{10} + \dot{m}_{12}h_{12} = \dot{m}_{13}h_{13} \tag{7}$$

Finally, for the first and second heat exchangers (or Boiler-1 and Boiler-2), the energy and mass balance equations give:

$$\dot{m}_{PTC}.\Delta h_{PTC} = \dot{m}_{13}(h_{14} - h_{13}) \tag{8}$$

$$\dot{m}_{WI}.\Delta h_{WI} = \dot{m}_1(h_1 - h_{14}) + (\dot{m}_2 - \dot{m}_{ph1})(h_3 - h_2) \tag{9}$$

For fulfilling the simulation of the performance of the power plant based on the above presented system-level model, one needs to have a thorough detailed model and explanation of the solar collectors and the incineration process. These are discussed hereunder.

The PTCs: The PTC is one of the most common types of solar concentrating technologies for high-temperature applications. The PTCs comprise a reflector with a parabolic shape to reflect solar radiations on a receiver pipe. The receiver that carries the working fluid of the solar system is usually covered with an evacuated glass enclosure to minimize the heat losses. To predict a PTC behavior, an accurate study has been accomplished by the NREL (National Renewable Energy Laboratory) of America [29]. This report describes the development, validation, and use of a heat transfer model that determines the performance of a PTC with a linear receiver. In this report, a sort of simulations has been done for various physical conditions and characteristics of the PTCs and the accuracy of the calculations has been investigated. The base of thermal design of the PTC is on the calculations of trough focal point, rim angle, and concentration ratio. Figure 2-left shows the one-dimensional steady-state energy balance for the cross-section of a PTC linear receiver. Figure 2-right shows the thermal resistance model of the PTC.

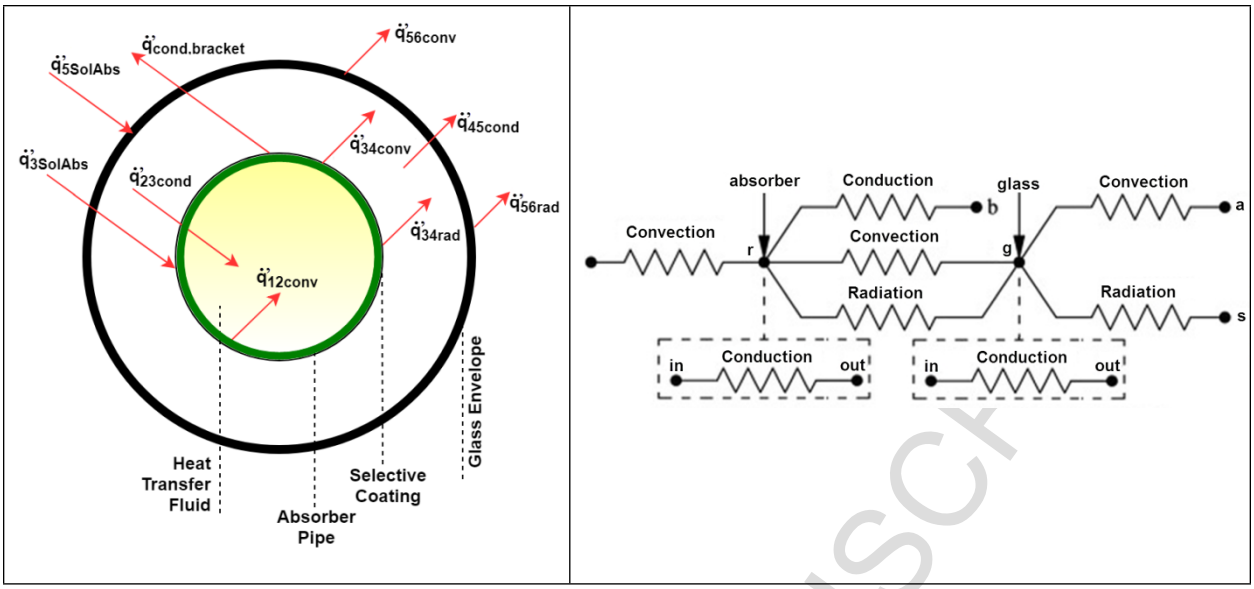

Figure 2 – Schematic of a PTC collector central pipe, a flow diagram of irradiation rays (left); the thermal resistance circuit (right) [30].

There are a large number of references with detailed mathematical model of solar irradiation availability and the net heat output of a PTC collector [31, 32]. As such, a detailed formulation of various sun tracking methods can be found in [33]. Therefore, a brief model of such collector is presented. Using the information given in Figure 2 and considering the basic solar engineering formulations, the energy balance equations for the unit length of the receiver will be as below:

$$q'_{12conv} = q'_{23cond} \tag{10}$$

$$q'_{3SolAbs} = q'_{34conv} + q'_{34rad} + q'_{23cond} + q'_{cond,bracket} \tag{11}$$

$$q'_{34conv} + q'_{34rad} = q'_{45cond} \tag{12}$$

$$q'_{45cond} + q'_{5SolAbs} = q'_{56conv} + q'_{57rad} \tag{13}$$

$$q'_{HeatLoss} = q'_{56conv} + q'_{57rad} + q'_{cond,bracket} \tag{14}$$

In which, each of the heat transfer terms is calculated from their specific formulations. These heat transfer terms are discussed hereunder.

Convective heat transfer between the working fluid of the solar system and the absorber (q'_{12conv}): this term may be given by:

$$q'_{12conv} = h_1 D_2 \pi (T_2 - T_1) \tag{15}$$

where, h_1, D_2, T_1, T_2 are the internal convective heat transfer coefficient at T_1, the internal diameter of the absorber pipe, mean temperature of the working fluid, the internal surface temperature of the absorber pipe, respectively. From simple heat transfer equations, h_1 is calculated by:

$$h_1 = \frac{k_1 Nu_{D2}}{D_2} \tag{16}$$

in which, Nu_{D2} and k_1 are respectively the Nusselt number and the thermal conductance of the working fluid at T_1. At typical operating conditions, the regime of flow through the receiver is turbulent for which Nusselt number is calculated by [34]:

$$Nu_{D2} = \frac{f_2/8\left(Re_{D2} - 1{,}000\right)Pr_1}{1 + 12.7\sqrt{f_2/8}\left(Pr_1^{\frac{2}{3}} - 1\right)}\left(\frac{Pr_1}{Pr_2}\right)^{0.11} \tag{17}$$

$$f_2 = \left(1.82 log_{10}\left(Re_{D2}\right) - 1.64\right)^{-2} \tag{18}$$

where, f_2, Pr_1 and Pr_2 are the friction factor for the inner surface of the absorber pipe, Prandtl number at the working fluid temperature and Prandtl number at the absorber inner surface temperature.

Conductive heat transfer through the absorber wall (q'_{23cond}): this term can simply be calculated as [35]:

$$q'_{23cond} = 2\,\pi k_{23}(T_2 - T_3)/\ln\,(D_3 - D_2) \tag{19}$$

where k_{23}, T_2, T_3, D_2 and D_3 are the absorber thermal conductance at the average absorber temperature, the absorber internal surface temperature, the absorber external surface temperature, the absorber internal and external diameters, respectively.

Heat transfer from the absorber to the glass envelope (q'_{34rad}): This space is to be fully vacuum and the only heat transfer mechanism will be radiation. The radiative heat transfer between the absorber and the glass envelope is calculated by [35] :

$$q'_{34rad} = \frac{\sigma\pi D_3(T_3^4 - T_4^4)}{(1/\varepsilon_3 + (1 - \varepsilon_4)D_3/(\varepsilon_4 D_4))} \tag{20}$$

in which, σ, D_4, T_4, ε_3 and ε_4 are Stefan-Boltzmann constant, the inner glass envelope diameter, the inner envelope surface temperature, the absorber selective coating and the glass emissivity factors, respectively.

Conductive heat transfer through the glass envelope (q'_{45cond}): The envelope is made of Pyrex glass. Here, according to [36], this term is assumed as a constant value of 1.04 W/m^2.

Heat transfer from the glass envelope to the atmosphere (q'_{56conv} and q'_{56rad}): Here, there are two heat transfer mechanisms of the convection to the environment and the radiation to the sky. The former is assumed to be forced (wind blowing) and the latter is due to the temperature difference between the glass envelope and the sky. For the convective term, one has:

$$q'_{56Conv} = h_{56} D_5 \pi (T_5 - T_6) \quad (21)$$

$$h_{56} = \frac{k_{56} Nu_{D5}}{D_5} \quad (22)$$

$$Nu_{D5} = C Re_{D5}^{m} Pr_6^{n} \left(\frac{Pr_6}{Pr_5}\right)^{1/4} \quad (23)$$

where, T_5, T_6, h_{56}, k_{56} and Nu_{D5} are the glass envelope outer surface temperature, the ambient temperature, convective heat transfer coefficient of air, air thermal conductance, the glass envelope outer diameter and the average Nusselt number based on the glass envelope outer diameter given by the Zhukauskas' correlation, respectively. In the Nusselt number correlation, the values of the constant coefficients of *C* and *M* depend on the Reynolds number of the airflow around the envelope surface as below:

Re_D	C	M
1-40	0.75	0.4
40-1,000	0.51	0.5
1,000-20,000	0.26	0.6
20,000-100,000	0.076	0. 7

Also, the value of *n* will be 0.37 if *Pr* <= 10; otherwise, *n*=0.36. As such, the net radiative heat transfer rate will be calculated by the same correlation as that of the absorber-envelope.

The equation for the solar absorption in the glass envelope is:

$$q'_{5SolAbs} = q'_{si} \eta_{env} \alpha_{env}; \quad \textbf{where: } \eta_{env} = \varepsilon'_1 \varepsilon'_2 \varepsilon'_3 \varepsilon'_4 \varepsilon'_5 \varepsilon'_6 \rho_{cl} K \quad (24)$$

in which, q'_{si}, η_{env}, α_{env} and K are solar irradiation per receiver length, the effective optical efficiency at the glass envelope, the absorptance of the envelope and the incidence angle modifier, respectively.

Finally, the rate of solar energy absorbed by the absorber is given by [31,32]:

$$q'_{3SolAbs} = q'_{si} \eta_{abs} \alpha_{abs}; \quad \textbf{where: } \eta_{abs} = \eta_{env} \tau_{env} \quad (25)$$

where, η_{abs}, α_{abs} and τ_{env} are the effective optical efficiency at absorber, the absorptance of the absorber and the transmittance of the envelope, respectively.

The WI Unit: WI is done for a variety of purposes and is used as a treatment for a very wide range of wastes. The recovered energy from a WI process can produce electricity, steam, or heat. In this work, the waste is incinerated for producing heat at high enough temperature for running a Rankine cycle. In the

production assessment process, the amount of waste for burning and supplying the required energy of the power plant is determined. One of the ways by which the amount of the released energy in the waste incinerators (and subsequently received by the thermal power plant) can be calculated is the use of an average lower heating value (LHV) for the waste source. For this purpose, the waste should be well mixed and homogeneous. Thus, by burning a certain amount of waste, the amount of available energy can be estimated. In this paper, the LHV of waste (LHV_{wst}) is considered as 8,100 kJ/kg [37]. In addition, the incineration process has also an efficiency (η_{wi}), which is in the range of 70-80%. In this work, the uniform efficiency of 80% has been considered for the incineration process (η_{wi}). Having said this, one can calculate the amount of heat released in such a process as:

$$\dot{Q}_{wi} = \eta_{wi} \dot{m}_{wst} LHV_{wst} \tag{26}$$

in which, $\dot{m}_{wst}$ refers to the mass flow rate of the waste.

In the end, Figure 3 presents a flowchart of the step-by-step instruction of how these equations are used for modelling the performance of the proposed hybrid system.

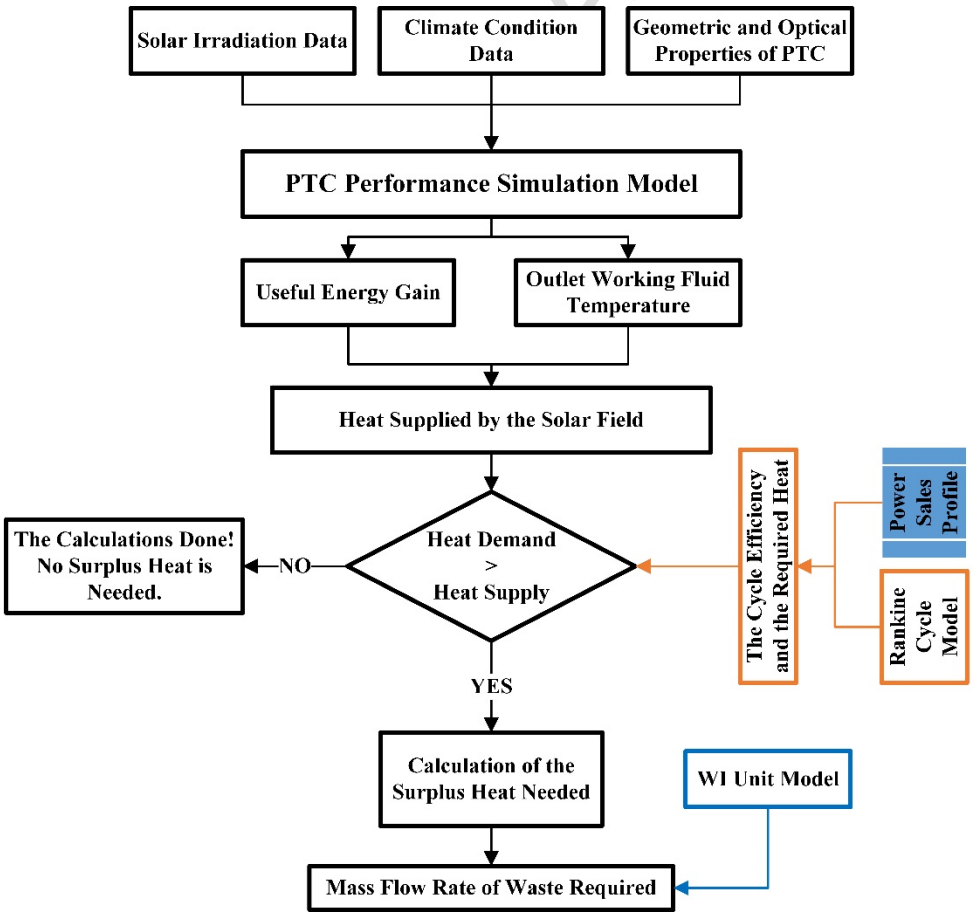

Figure 3 – A flowchart of the hybrid system modelling steps.

Emission Calculation: Naturally, a solar power plant is 100% environmentally friendly with no emission and the WI unit is the only part of the system that may cause pollution. This is, however, a coin with two sides, that is, the source of energy in a WI unit is municipal waste that is to be landfilled otherwise. According to the report released by the US Environmental Protection Agency [38], the greenhouse gas emissions from a total of 137.7 million tonne waste landfilled in 2015 amounted to 115.7 million tonnes of CO_2 equivalent (CO_2e). This gives an average emission value of 840 kg CO_2e per tonne of landfilled municipal waste while the emission when incinerating the waste is far less. Mathematically, the amount of CO_2e emission in a WI process might be calculated by [39]:

$$E_{CO_2e} = \sum E_\lambda GWP_\lambda \tag{27}$$

where, E_λ is the emission of different types of greenhouse gases such as CO_2, N_2O, etc., GWP_λ is the global warming potential of the given greenhouse gas type compared to the pollution of CO_2 (tonne of CO_2/tonne of the considered gas). The emission of each gas from a WI process is calculated by [39]:

$$E_\lambda = \sum \mu_\lambda \xi M \tag{28}$$

where, μ_λ is the emission concentration of the given gas, M is the mass of the waste and ξ is the exhaust gas volume. The values of M, ξ and GWP could be calculated by the guidelines given in the literature. Based on the recommendation given in [39], in this study, an average emission of 415 kg of CO_2e for the incineration of 1 tonne of municipal solid waste is taken into account.

3. Case Study

In this section, a detailed information about the availability of solar energy at the case study, the specific characteristics of the hybrid system, the solar collectors employed and the WI unit is presented. Table 1 details the main technical characteristics of the Rankine cycle.

Table 1 – The Rankine cycle technical information

Parameter (unit)	Value/information
Nominal capacity (MW)	10
Working fluid (-)	Steam/water
Inlet HPT temperature (°C)	500
Inlet IPT temperature (°C)	500
Inlet LPT temperature (°C)	350
Inlet HPT (MPa)	10
Inlet IPT Pressure (MPa)	3

Inlet LPT pressure (MPa)	0.25
Condenser pressure (kPa)	10
Boiler thermal efficiency (%)	95
Turbine isentropic efficiency (%)	85
Pump isentropic efficiency (%)	85
Electricity generator efficiency (%)	95

Table 2 presents information about temperature, pressure, enthalpy and mass flow rate of the working fluid of the Rankine cycle.

Table 2 – Thermodynamic properties of the working fluid in various points of the Rankine cycle.

Point	P (bar)	T (K)	h (kJ/kg)	$\dot{m}_{nominal}$ (kg/s)
1	100	773.2	3,374.0	10.772
2	30	622.8	3,113.9	10.77
3	30	773.2	3,456.6	9.016
4	2.5	573	3,069.8	1.09
5	0.1	318.9	2,583.1	7.926
6	0.1	318.9	191.72	7.926
7	2.5	319	192.04	7.926
8	2.5	400.6	535.39	9.016
9	100	402.3	549.23	9.016
10	100	507	1,007.2	9.016
11	30	507	1,008.2	1.756
12	100	509.2	1,019.6	1.756
13	100	522.6	1,082.0	10.77

Table 3 details the physical characteristics of the LS-2 PTC assembly used in the hybrid system [29]. This module has been widely used in previous studies.

Table 3 – The characteristics of the LS-2 PTC assembly.

Parameter	Symbol	Value
Width of the PTC	W	5 m
Length of the PTC	L	7.8 m
Focal distance of the PTC	F	1.71 m
Aperture of the PTC	A_a	39.0 m^2
Concentration ratio of the PTC	C	22.74
Receiver inner diameter	D_{ri}	66×10^{-3} m
Receiver outer diameter	D_{ro}	70×10^{-3} m
Cover inner diameter	D_{ci}	109×10^{-3} m
Cover outer diameter	D_{co}	115×10^{-3} m
Receiver inner surface	A_{ri}	1.617 m^2
Receiver outer surface	A_{ro}	1.715 m^2
Cover inner surface	A_{ci}	2.671 m^2
Cover outer surface	A_{co}	2.818 m^2
Receiver emittance	ε_r	0.2
Cover emittance	ε_c	0.9
Absorber absorbance	α_{abs}	0.96
Cover transmittance	T	0.95
Concentrator reflectance	r_{conc}	0.83
Incident angle modifier	IAM	1
Number of series PTCs in each assembly	-	6
Maximum working fluid mass flow rate	$\dot{m}_{swf}$	9.54 kg/s
Working fluid line pressure	P_{swf}	0.85 MPa

Finally, Table 4 lists the main technical features of the WI unit.

Table 4 – The WI unit main features.

Item	Information/value
Type of waste	Municipal solid waste
Efficiency of incineration process	80%
LHV of the waste	8,100 kJ/kg
Working flow	Water

The case study of this work is a solar plant in Aarhus, Denmark, with an altitude of 56°. Figure 4 gives information about the hourly averaged solar irradiation available on a horizontal surface measured in the case study [40]. The figure is presented in two different panels for the first and second six-months of the year. As seen, a maximum of about 850 W/m^2 solar energy is expected on a horizontal surface during the summertime, while the irradiation during the wintertime is rather small. This is due to the geographical location of Aarhus with its very high latitude as well as the very cloudy weather of the city, especially during the fall and winter.

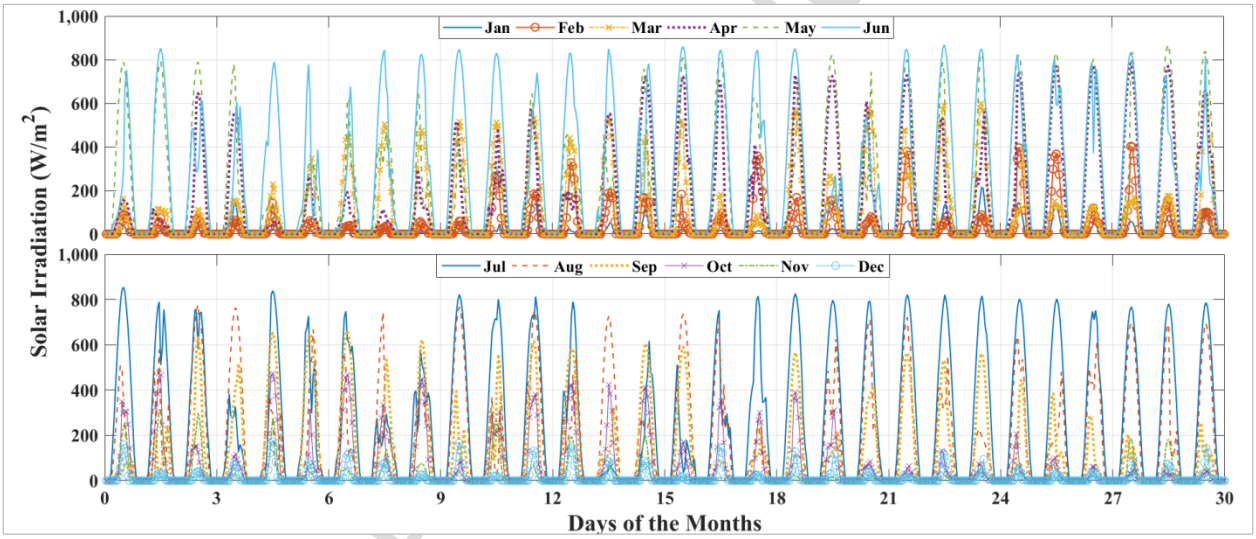

Figure 4 - Solar irradiation on a horizontal surface in the case study [40].

Figure 5 presents a comparison of the solar irradiation on a horizontal surface and a tracking plate both with 1 m^2 area, for three randomly selected days of hot (July), cold (January) and moderate (March) months of the year in the case study. The irradiation received by a tracking plate is calculated based on the irradiation on a horizontal surface [40] and the correlations governing on the sun-trackers [33]. Note that although the simulation has been done for the entire year, a few days are chosen for the presentation of the results to enable the readers to track the variation of the parameters over time. This figure aims at showing the effect of employing the tracking system for the solar field. As seen, there is a remarkable difference between what is received with the horizontal surface and that of the tracker early in the morning and late in the afternoon.

This effect is more of importance during the summer when the sun is more available, where a better collection performance makes a bigger difference.

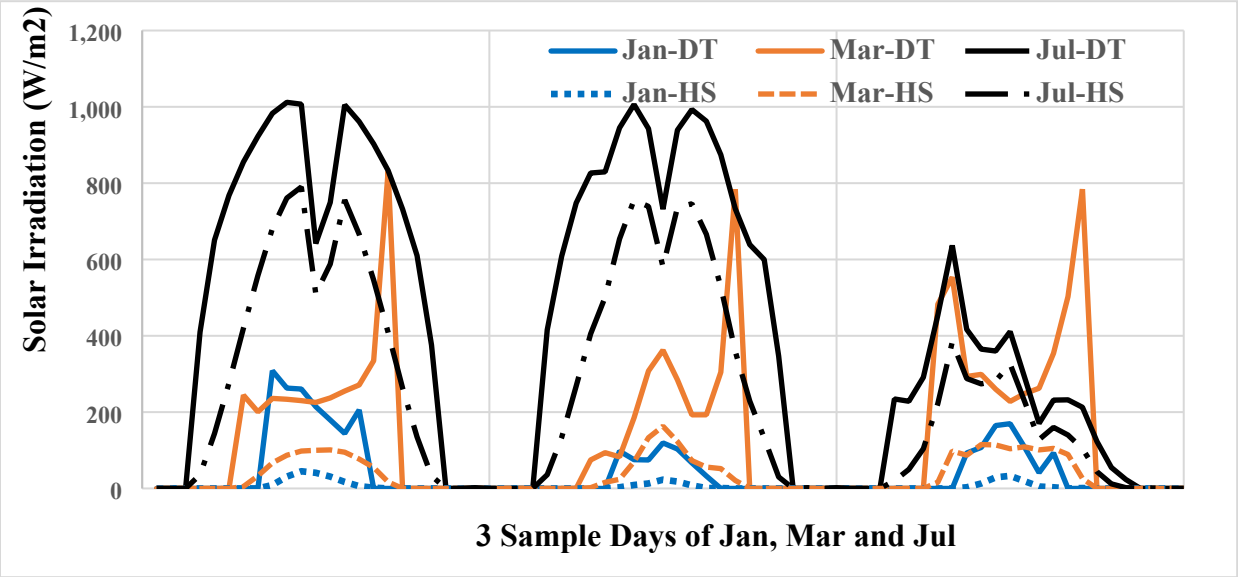

Figure 5 - Comparison of solar irradiation on a horizontal plane and a tracker for three sample days in three months.

4. Results and Discussion

In this section, the results of the simulation carried out on the proposed hybrid system will be presented. For a better understanding of the proficiency of the hybrid cycle, three different scenarios will be evaluated. First, it is assumed that the power plant is supposed to be supplied by solar PTCs and a year-round performance analysis of the plant is carried out. In the second scenario, it is presumed that the heat demand of the steam power plant is provided by a WI unit, with no solar collector as back up. Finally, the results obtained from the above scenarios will be compared with the results given for the hybrid plant.

Before going through the results of the simulations of the solar collectors, one should validate the model used for this purpose. For this, the results obtained from the developed model are compared with the experimental results presented in [29]. Table 5 gives the results of this examination for various conditions, i.e. different ambient temperatures; the inlet temperatures and velocities of the working fluid of the solar system, and solar irradiations. The output of the model is the outlet temperature of the working fluid of the solar system, which should be compared with the experimental output temperatures. As seen, the maximum deviation is only 0.1%, while the mean deviation value of the four cases is as small as 0.06%, is observed which proves the very high accuracy of the developed model for various operating conditions.

Table 5 – The results of the validation of the model developed for the PTC performance simulation.

Case	G_b (W/m^2)	T_{amb} (K)	T_{in} (K)	V(m^3/s)	T_{out} of the Exp. (K)	T_{out} of Model (K)	Deviation (%)
1	933.7	294.35	375.35	47.7	397.15	397.44	0.073
2	968.2	295.55	424.15	47.8	446.45	446.776	0.073
3	982.3	297.45	470.65	49.1	492.65	492.709	0.012
4	909.5	299.45	523.85	54.7	542.55	541.966	0.108

It is noteworthy that the model is validated for the severest case of G=982.3 W/m^2 and T_{in}=523 K resulting in an outlet temperature of around 542 K because the reference work does not report any experimental results for a sharper condition. However, since so accurate responses are given for the lower temperatures and solar irradiations by the simulation results and as the methodology is just the same, one may conclude that the simulation model developed for the PTCs is quite reliable.

Figure 6 presents the profile of the hourly averaged produced heat by a tracking PTC assembly out of the received solar irradiation for the above sample days. The PTCs are based on the characteristics given in Table 2. As seen, a maximum of about 147 kW heat may be produced by each PTC assembly during the sample days of July and this maximum production level is quite small in January representative days, i.e. well below 40 kW.

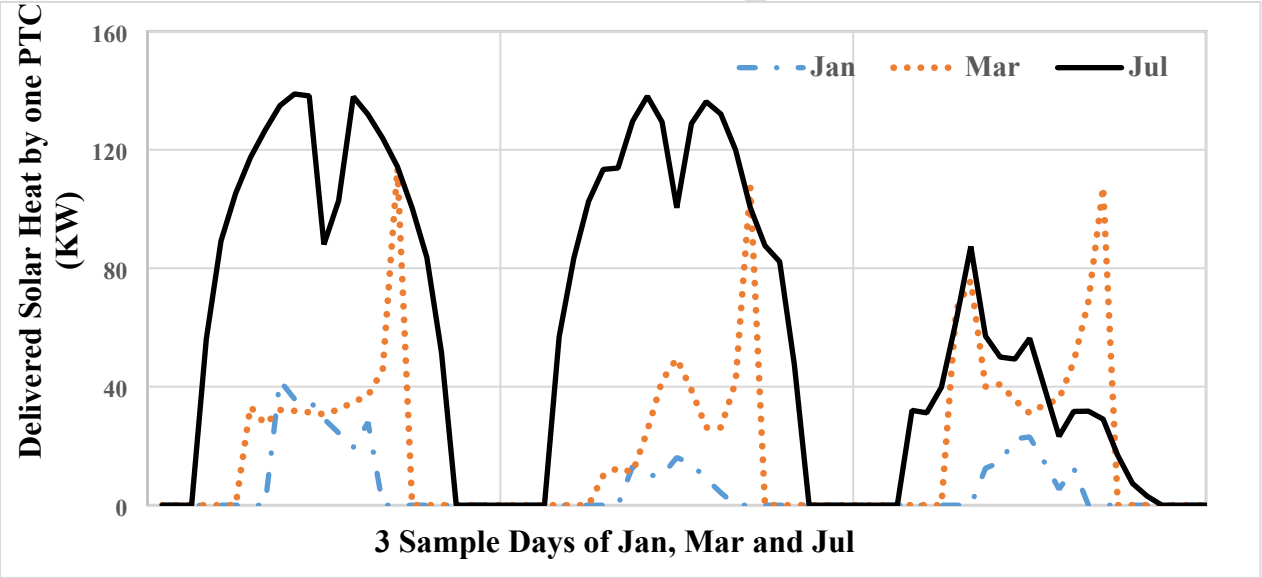

Figure 6 - Useful heat produced by a tracking PTC assembly over the sample days.

For sizing the components and assessing the overall performance of the steam power plant, one should have information about the capacity of the plant and the energy efficiency of the cycle. As discussed, a maximum capacity of 10 MW is considered for the power plant. Taking into account the characteristics considered for the power block of the plant as well as the thermodynamic relations governing on a Rankine cycle (detailed in the previous sections), one could find the overall efficiency of the cycle in nominal operation load as 36%. Thus, for deriving such a steam power plant, a heat source with the peak heat production of about 28 MW is required. Considering an overall efficiency of 0.95 for the heat exchanger transferring solar

heat to the Rankine cycle working fluid (steam), one can easily calculate that a total number of 200 LS-2 PTC assemblies with the characteristics detailed in Table 3 would be required for the solar power field.

Figure 7 shows how the outlet temperature of the solar collector array affects the efficiency and the level of delivered heat of the employed solar PTC assembly. As the figure shows, both the efficiency and the net heat deliverable with the PTC assembly will reduce by increasing the outlet temperature of the working fluid. For a low outlet temperature of 500 K, a thermal efficiency of 72% is achievable where the net heat producible is about 180 kW. On the other hand, when the temperature of the fluid is to increase to 1,000 K, the efficiency and net heat output will be 32% and 79 kW, respectively, though the working fluid of the solar system is to be heated up to a temperature of 550 °C (823.3 K).

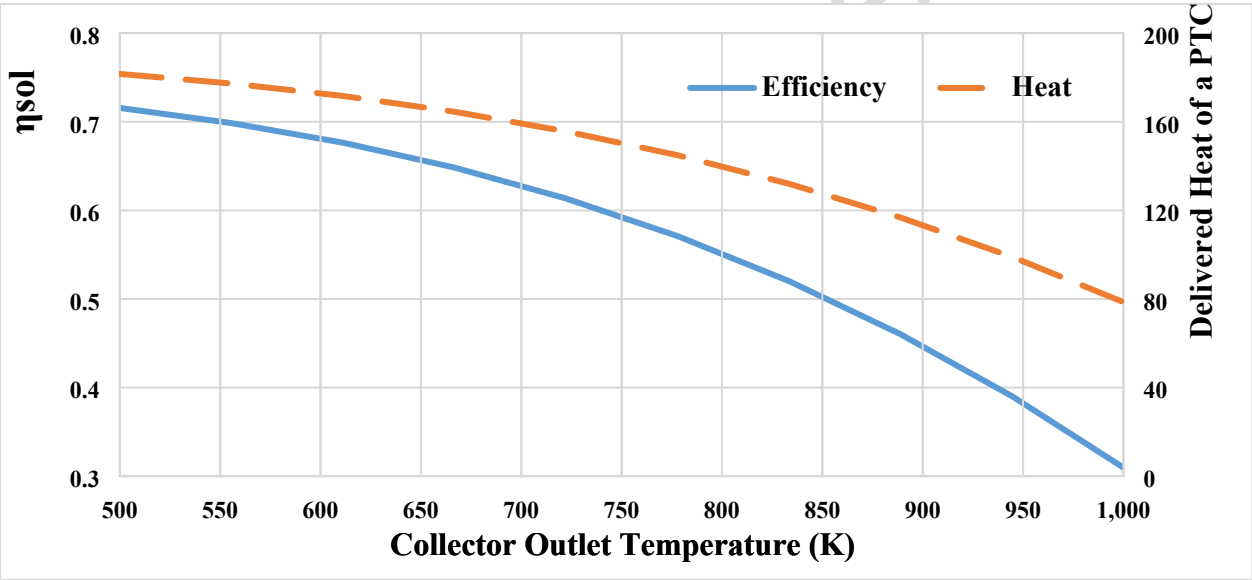

Figure 7 - The effect of outlet temperature on the PTC assembly thermal efficiency.

Regardless of the type of the power plant, in Denmark and probably anywhere else, the power plant should bid on an electricity sales profile for the entire of the next day. For renewable energy power plants, such as solar and wind plants, this profile is set based on the forecast data that the plant receives one day ahead. Finding the optimal power sales strategy requires professional optimization algorithms and is out of the scope of this work. Thus, just as a sample sales strategy, the power plant bids on the daily average amount of power predicted to be generated by the solar plant from the sunrise to the sunset. For example, if a total of 60 MWh power is predicted to be produced in a given day with 12 h length, the power plant bids on a uniform power sales value of 5 MW from sunrise to sunset. The power sales during the rest of the day will be zero always. Figure 8 shows the power sales pattern of the power plant based on this strategy over an entire year. As seen, the power plant will bid on the high uniform power sales of about 8 MW during the

sunshine hours in several days during the summer while this value will be as low as 0.2 MW for a few cases during the winter. Note that besides the level of power sales, the duration of the day is also a matter of importance which is extremely longer during the summer. This can be seen in Figures 5 and 6 in which the day representing January is much shorter than those March and especially July.

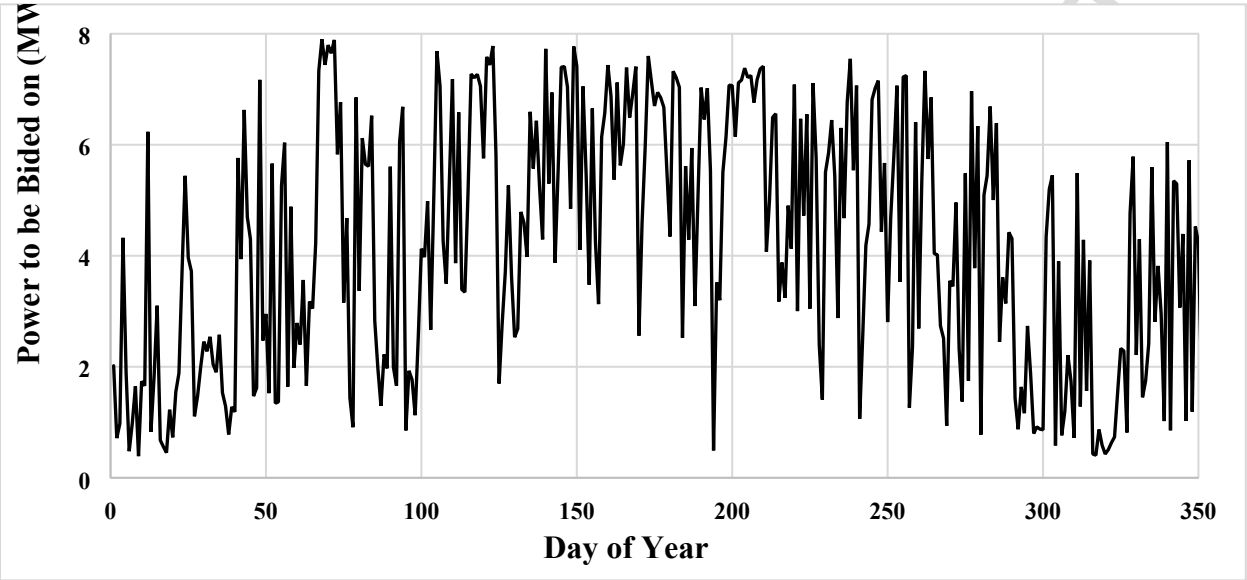

Figure 8 - The power sales strategy of the solar power plant.

Note that the set point of 500 ^{o}C for the high-pressure turbine inlet temperature (and 550 ^{o}C for the outlet working fluid of the PTCs) is made to control the mass flow rate of the working fluid of the solar collectors and the power cycle.

Naturally, if a renewable power plant is not accompanied with an auxiliary energy supply source, it should be equipped with an energy storage unit. For example, a battery as an electricity storage unit is the most common type of storage facility for a wind turbine or a PV farm [41]. For a solar thermal power plant, a thermal energy storage is required, which is usually a molten salt heat storage unit [42]. In this work, it is assumed that the solar thermal power plant is equipped with a molten salt heat storage system. Therefore, if the supplied heat is more than required, the surplus heat is stored in the heat storage unit for later use. In contrast, if there is not enough heat supplied, the stored heat is reclaimed from the storage unit. Clearly, in case of discharging the storage and lack of power to meet the bided value, there will be financial fines for the power plant. Figure 9 shows the rate of solar heat produced by the collector array (this is simply the result of multiplication of data given in Fig. 6 and the number of PTC assemblies in the solar field) versus the amount of heat required to produce the bided power for the sample days. It is reminded that there is no strategy for selecting these days and they are just randomly selected for the presentation of the results in a better resolution so that one could track the fluctuations of the given parameters over time.

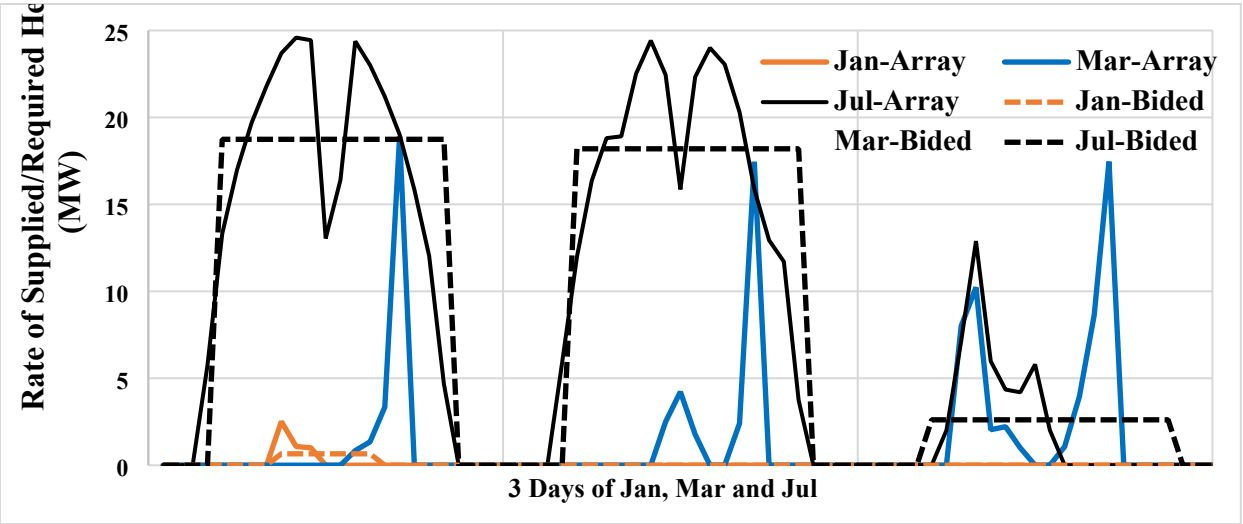

Figure 9 - The rate of produced solar heat and the heat needed for power production over the sample days.

As seen, during January representative days, it is only on the first day that something is expected from the solar plant and no heat is produced by the solar collectors. On the other hand, the first two sample days of July are quite productive and the solar collectors can be highly beneficial. In these days, little solar irradiation fluctuations are seen and a large amount of surplus heat is produced around noon. This surplus heat will be used to charge the storage unit and then be reclaimed to recover the heat demand late in the afternoon. One should note that in the figure above less heat production than that required for meeting the power sales strategy is produced during early day times. For such cases, the energy storage will take over the compensation of the heat shortage of the plant employing the excess surplus heat that it has received in the previous day. Figure 10 represents the rate of heat coming directly from the solar collectors versus the contribution of the storage unit in the heat production of the plant for the sample days along the year.

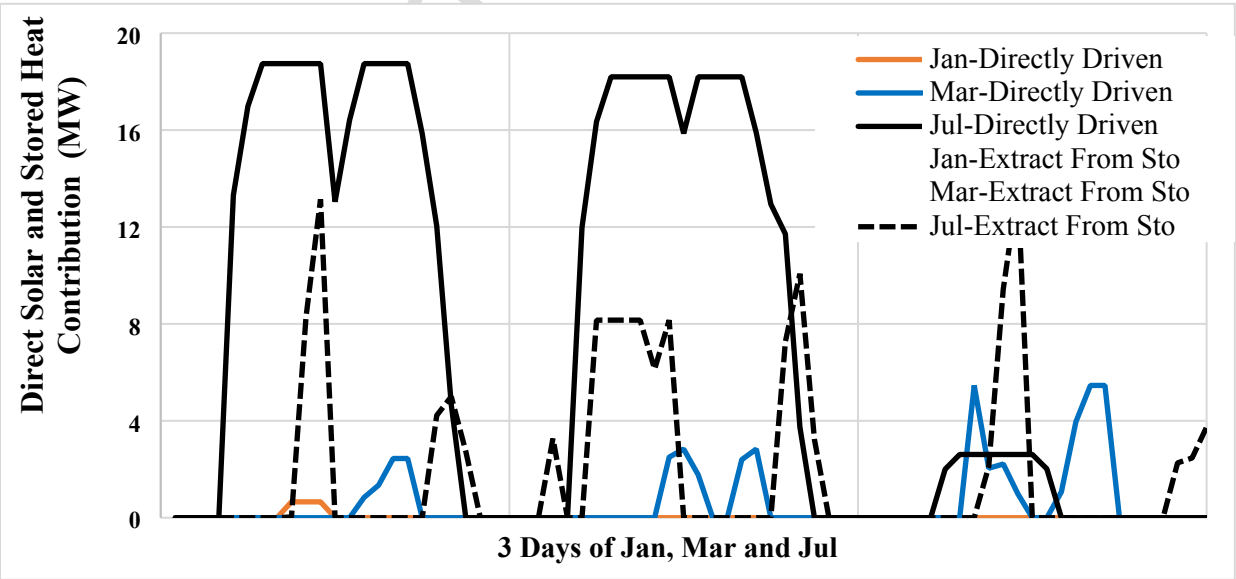

Figure 10 - The rate of direct solar heat preparation and heat provided via the storage unit for power production over the sample days.

Figure 11 shows the variation of the temperature of the storage tank for the entire year. Here, one could see when the charging and discharging processes take place. For a better understanding of the trend of the storage temperature variation, the magnified temperature profile of the storage for a duration of 24 hours has been brought along the annual temperature graph. As the storage unit is the source of heat production for the preheating process before the main boiler, which is driven by the solar collectors, the storage temperature does not go so high and fluctuates between 370 K and 490 K.

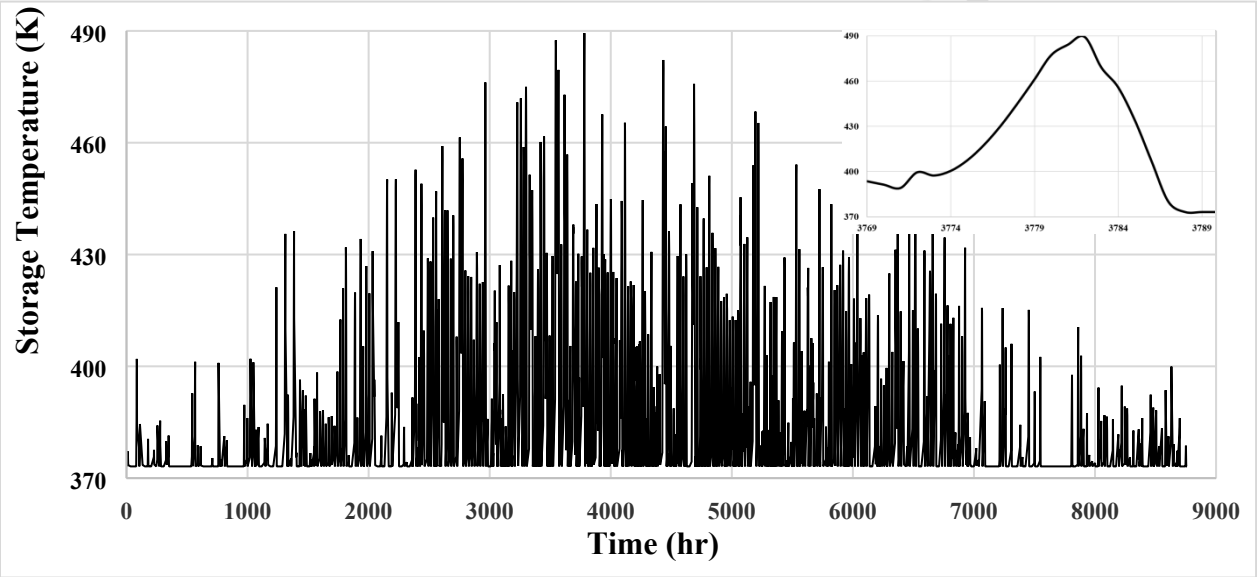

Figure 11 - The variation of the storage tank temperature during an entire year of operation of the solar power plant.

Figure 12 gives information about the amount of power output shortage of the system compared to the bided value, for which the power plant is to be fined. The figure is presented for one sample day in January, March, and July. This figure particularly presents the times during which the solar collectors could not provide sufficient energy for the Rankine cycle and the storage system is either fully discharged and unable of providing a backup heat flow for the system. The investigations show that a total annual of 19% of the bided value is missing in the power plant. This power shortage should either be recovered by an auxiliary heat production service or the power plant is financially fined.

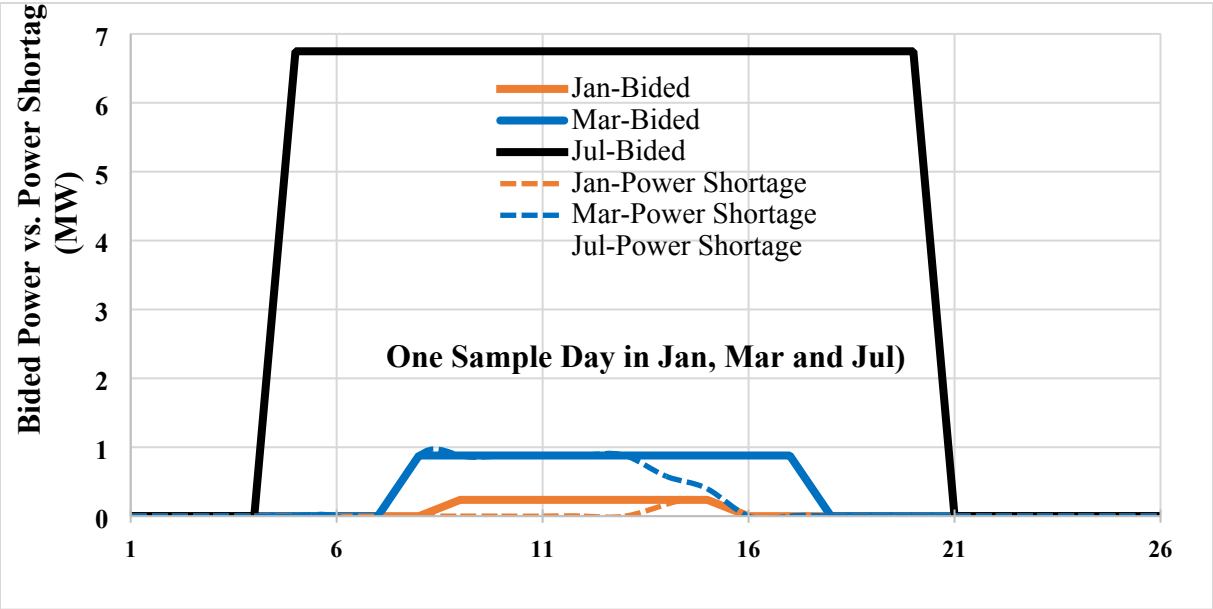

Figure 12 - The bided power vs. the power shortage of the plant for a few sample days along the year.

Since the efficiency of the collector array, as the heat production unit of the plant, depends on the solar irradiation and environmental parameters, a variable efficiency graph is obtained for the power plant along the year. Figure 13 shows the variation of the efficiency of the CSP steam power plant in an hourly averaged manner for the first and second 6-months of the year. The results show that a maximum of 55% efficiency is given for the solar system, the Rankine cycle efficiency by neglecting the off-design conditions shows a uniform efficiency of 36%, and the annual average energy efficiency of the whole CSP plant is 14%. Here, the annual efficiency of the system is defined as 'the value of the total amount of electricity produced by the solar power plant' divided by 'the total annual solar irradiation on the tracking PTCs'.

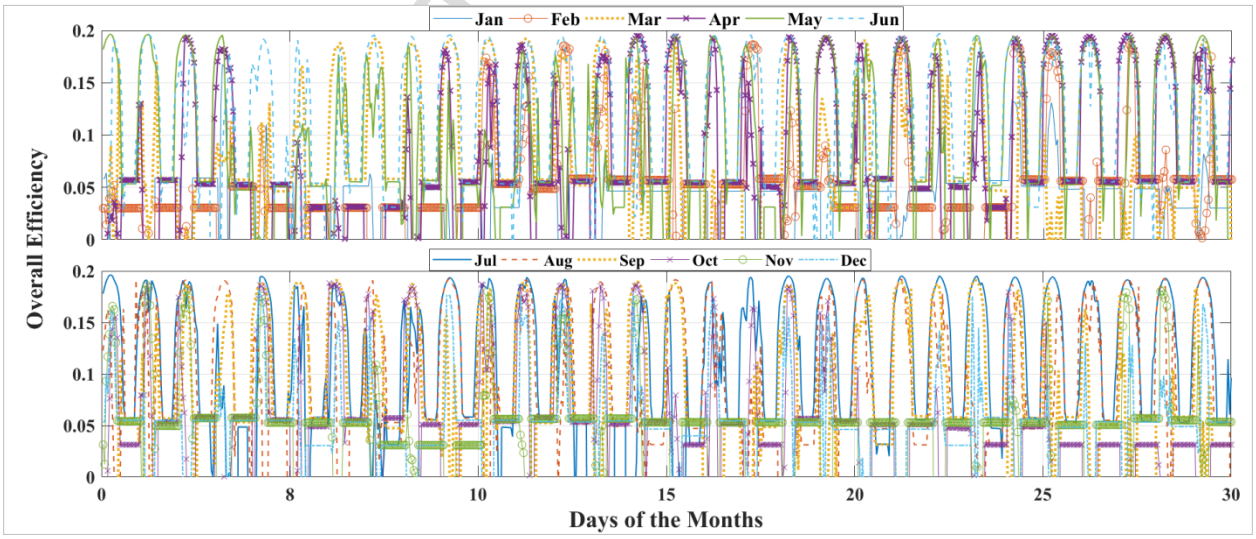

Figure 13 - The hourly averaged energy efficiency of the CSP plant along the year.

The second case is a WI driven steam power plant. Figure 14 shows the rate of waste mass required to cover the same power sales strategy as that committed in the solar-only driven plant (shown in Figure 8). Naturally, here, there will not be any penalty for the plant as the required fuel for power generation will always be available.

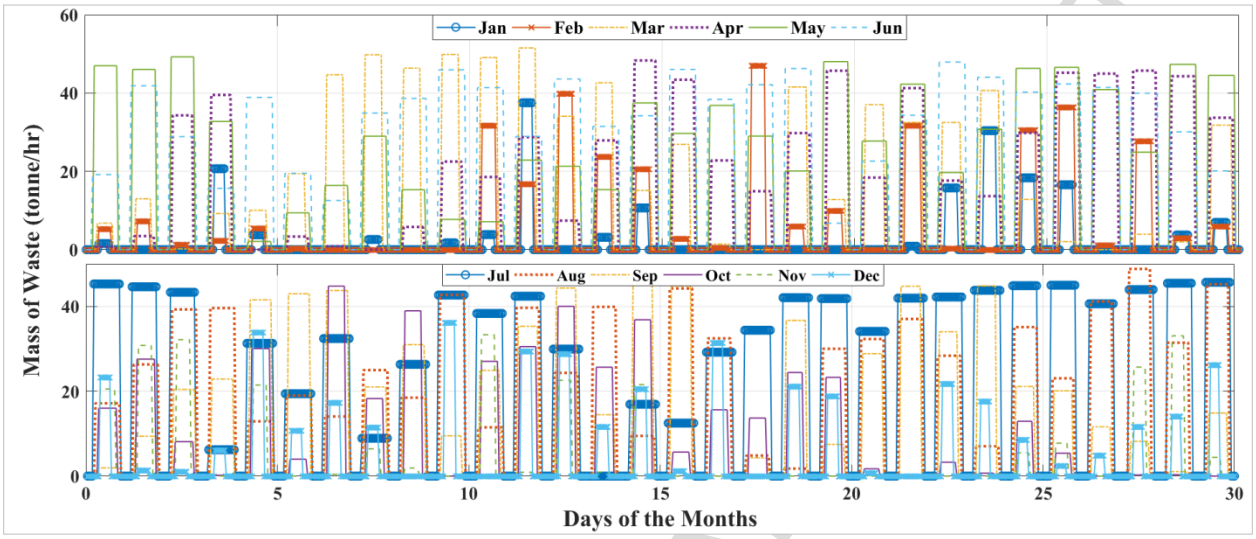

Figure 14 - The rate of the mass waste required in the WI plant.

Figure 15 shows the total monthly amount of CO_2e production by the WI plant for covering the given power sales pattern along the year. Naturally, as the previously defined power sales strategy was based on the availability of solar energy which is much better during the summer, the WI plant also has a more contribution during the summer and consequently, the rate of CO_2e emission of the plant is much more during this period.

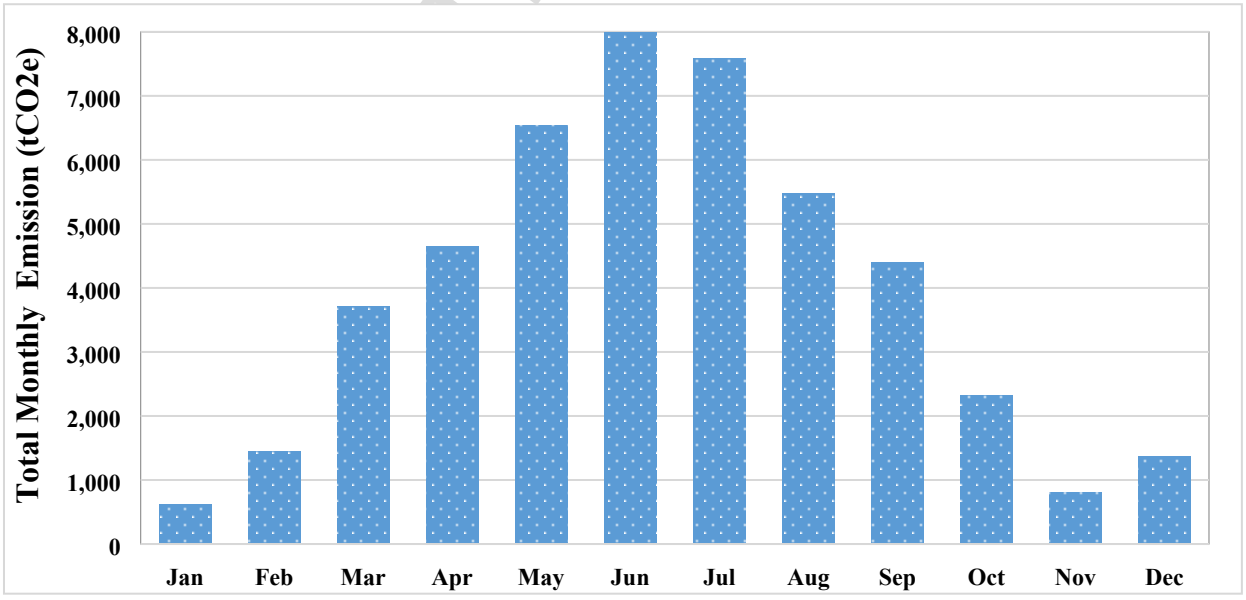

Figure 15 - The amount of total monthly CO_2e emission in the WI plant.

The third case is the proposed hybrid solar-WI power plant. One of the main advantages of this configuration is that the sales pattern can be modified so as not to be fined for any unsuccessful coverage of the committed power sales. In addition, the power plant could bid on higher power values, making a larger contribution to the grid with the same size of the solar field. Again, as a sample power sales strategy, a uniform power sales equal to the maximum daily producible solar power is proposed for the entire day (from the sunrise to the sunset). In this case, when the solar plant is working on its full capacity, the WI unit will be in standby mode and it comes into operation as the solar energy drops to fulfill the amount of power bided on during the day-ahead market. Figure 16 shows the power sales strategy of the combined plant. Expectedly, the maximum power sales of the hybrid plant is 10 MW as the solar thermal part is so sized that it could provide enough heat for the production of 10 MW of power in the sunniest day of the year. It is reminded that the power plant is supposed to provide electricity based on a uniform value along the day from sunrise to sunset. The comparison of this figure with Figure 8 clearly reveals how this secondary source of heat supply may increase the power supply potential of the CSP plant, and subsequently its reliability and economic incomes.

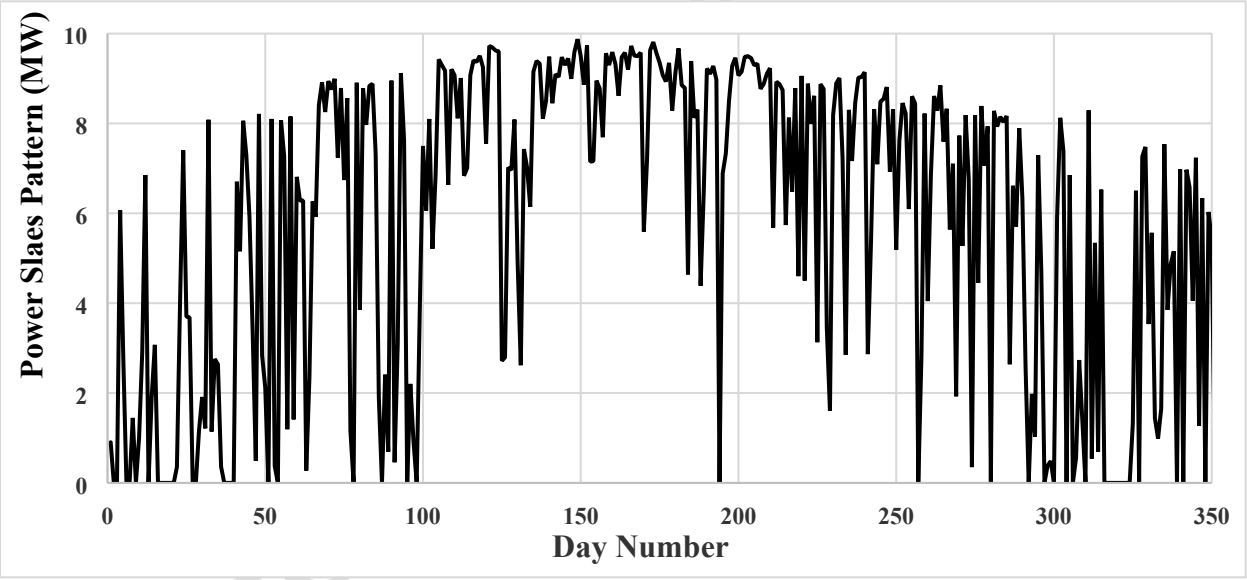

Figure 16 - The power sales pattern of the hybrid CSP-WI plant over the year.

Figure 17 shows the contribution of the solar field versus the WI unit in the heat production of the plant over a few sample days. As seen, during a given day, as the solar heat goes up, the WI heating duty decreases and vice versa. As seen, during January days, the power plant sales pattern is almost zero, because the solar irradiation availability is absolutely zero during these days.

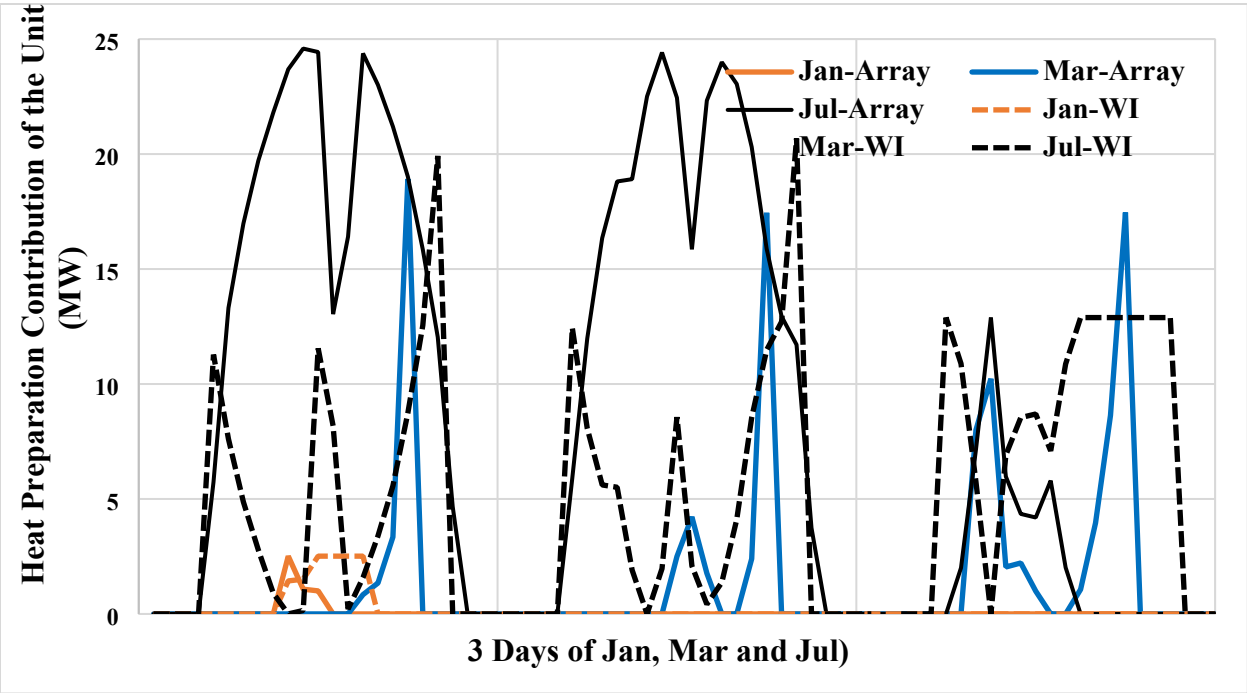

Figure 17 - The contribution of the solar PTCs and the WI unit to the heat production process of the power plant during a few sample days.

Figure 18 gives information about the total hourly mass of waste required for the incineration process in the hybrid power plant. According to the figure, the waste mass required is extremely higher during the summer days as based on the determined sales strategy; the plant would bid on a higher 24-hour power sales value in a sunnier day. Clearly, out of the bided value, during the sunshine hours, the solar thermal part will significantly contribute to the heat supply process while during cloudy hours the WI unit contribution would increase proportionally. As such, during the night hours, the WI unit is the only source of heat production of the plant as there is no solar energy available.

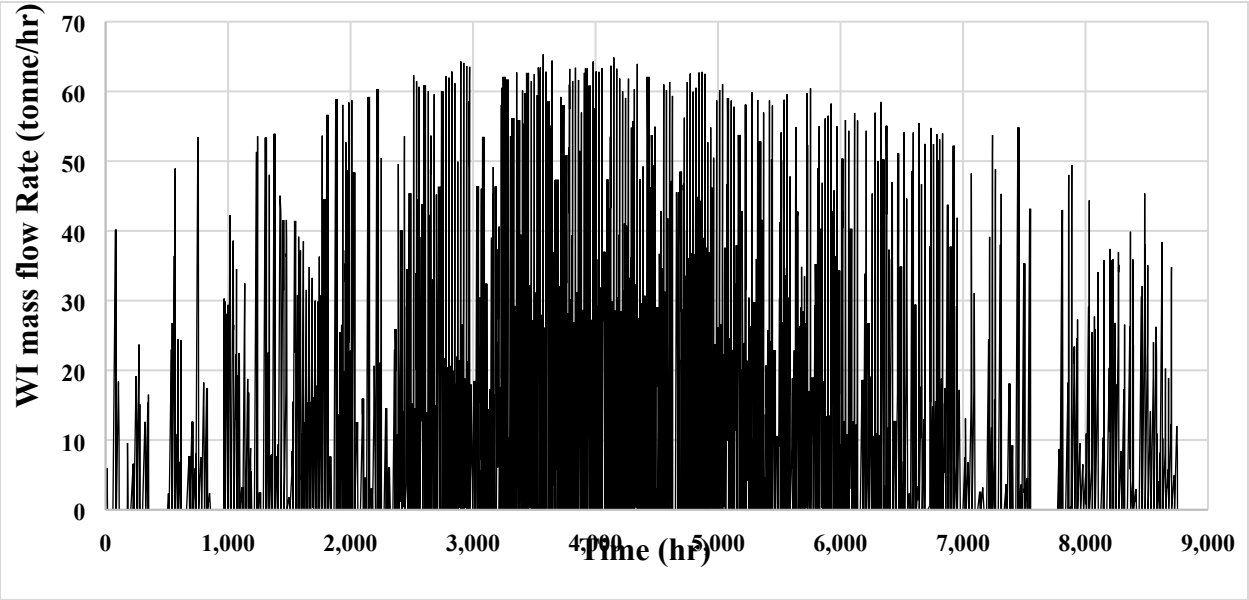

Figure 18 - The required mass of waste for the WI unit for covering the sales pattern values along the year.

Figure 19 gives information about the overall energy efficiency of the hybrid power plant. This graph is presented for a few sample days to be able to follow the trend of energy efficiency. It is noteworthy that, based on the recommendation coming from [35], the incineration process efficiency has been considered as 80%. Here, the statistics show that the overall annual energy efficiency of the hybrid plant is 24%. The total annual efficiency of the hybrid system is defined as the ratio of 'the total amount of electricity successfully produced by the power plant over the whole year' to 'the total energy supplied to the hybrid system (i.e. the summation of the solar energy irradiated on the PTCs and the energy given to the WI unit in form of municipal solid waste as the fuel)'.

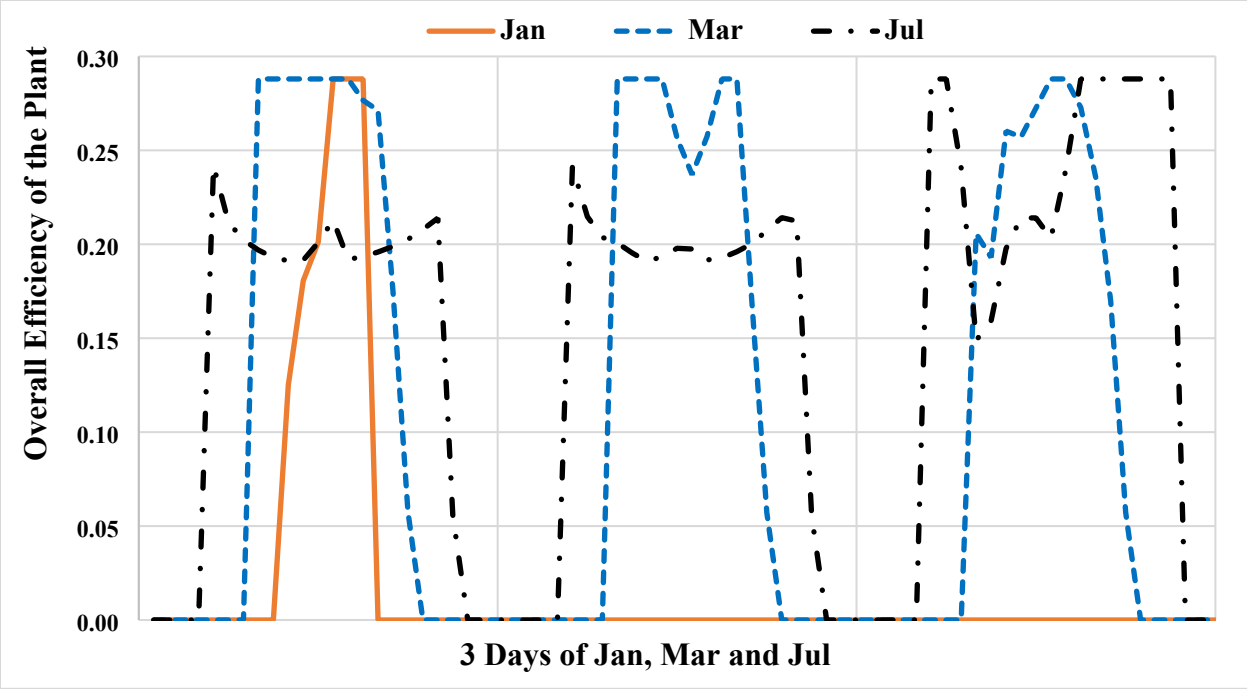

Figure 19 - The energy efficiency of the hybrid power plant over the sample days.

Figure 20 makes a comparison of CO_2e emission in the hybrid plant and the WI plant, based on the percentage of the net power produced. In other words, this figure gives the total daily CO_2e emission of the hybrid plant and gives an overview of the emission level if the WI unit was the only source of heat production for covering the power sales strategy shown in Figure 16. Here, two points are very important. The first point is the very significant emission reduction that the solar thermal system causes in the power plant. This difference is extremely larger during the warmer months of the year during which more solar energy is available, though the effect of the hybrid system is still remarkable during the wintertime.

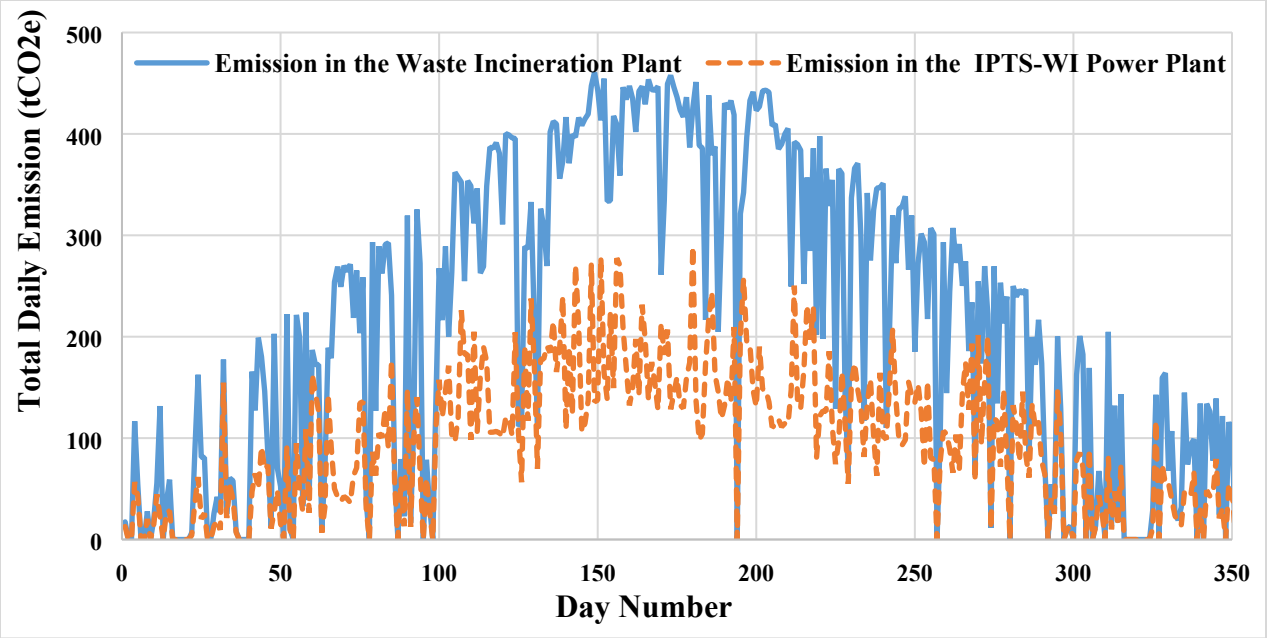

Figure 20 - Comparison of the CO_2e emission of the hybrid plant and a WI plant for the same power sales pattern.

The second important point is the amount of emission reduction that the hybrid power plant can make in comparison with a regular Rankine based power plant with a fossil fuel, e.g. natural gas. This is important because a WI unit, which is an active part of the proposed hybrid plant, offers the very valuable service of municipal waste management as the most environmentally friendly solution among all the waste management methods. Therefore, it is fair to consider the realistic environmental impact of the plant, which is preventing much greenhouse emission from landfilling. Based on the presented information, the prevented emission via incineration is 425 kg CO_2e (i.e. 840 – 415) per tonne of waste. Having this value, Figure 21 presents a comparison of the environmental impact of the proposed hybrid power plant compared to that of a natural gas-based Rankine cycle in a total monthly manner.

For calculating the amount of emission from the gas-based Rankine cycle, one only needs to calculate how much natural gas is burnt to cover the same power sales pattern by the Rankine cycle. Then,

$$\dot{m}_{ng} = \frac{\dot{Q}_{req}}{\eta_{blr} LHV_{ng}} \tag{29}$$

where, $\dot{m}_{ng}$ is the mass flow rate of the natural gas to be burnt, and $\dot{Q}_{req}$ is the required heat to be effectively produced by the boiler. A rough value for natural gas lower heating value (LHV) is 54,000 MJ/kg, and the boiler efficiency (η_{blr}) is considered as 95% [43]. Then, the emission of the system will be calculated by

simply multiplying the mass flow rate of gas consumed by the amount of CO_2e released per kg of gas burnt (i.e. 23.2 kg CO_2e per 1 kg of natural gas [44]).

As seen in the figure, there is a remarkable difference between the results, where the negative emission in the hybrid plant makes it a very interesting solution compared to the gas cycle in which a large amount of greenhouse gases is emitted. Note that the gas-based Rankine cycle power plant has been considered for a comparison because it is one of the main components of the global power system, probably more than any other technologies. The objective is to show how big is the emission difference when the conventional energy system is moving toward a smart energy system in which WI technology and renewable technologies are broadly used. This difference will even be much more significant when other fuel based technologies, e.g. gas turbine or Rankine cycle with coal as fuel, are considered because natural gas causes the least environmental impacts compared to any other fossil fuels.

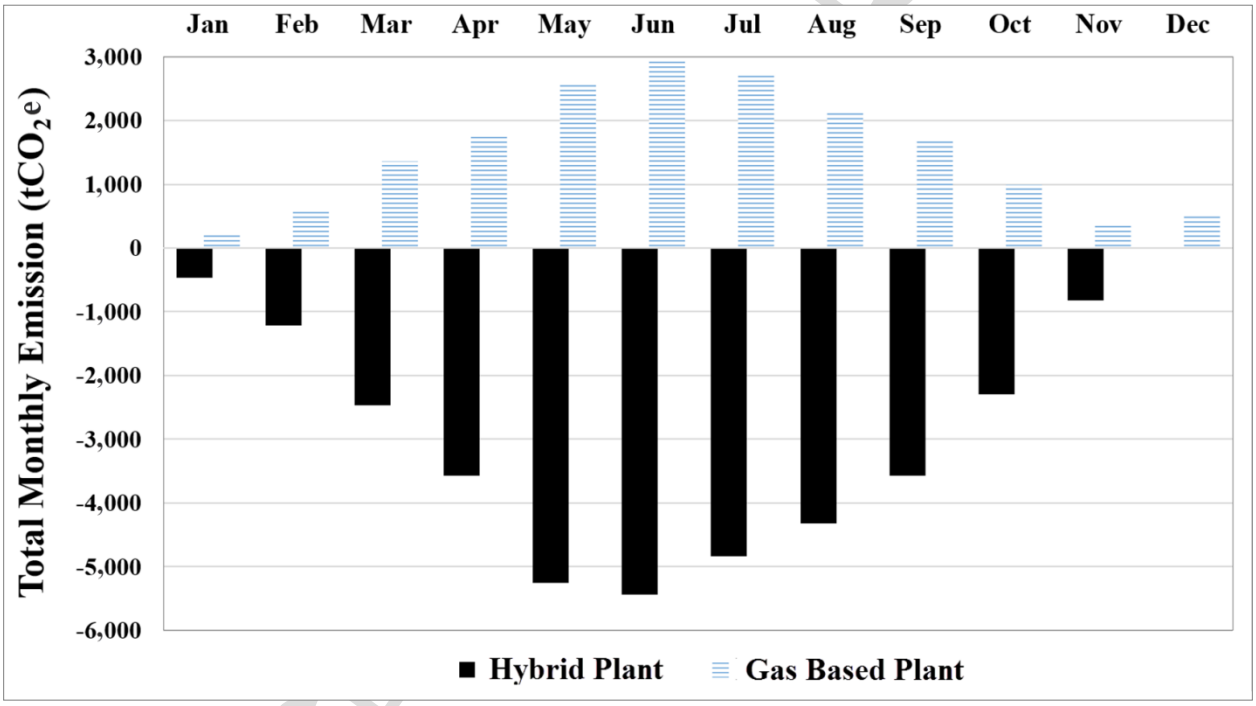

Figure 21 - Comparison of the CO_2e emission of the hybrid plant and a natural gas power plant.

In the end, it is underlined that the variable source of energy in a solar power plant and the not perfectly accurate forecast data that such a power plant gets about the availability of the solar irradiation in the coming 24 hours, makes the performance of the solar power plant challenging in the day ahead power market. One solution for this is employing electricity storage systems that are too costly and suffer from technical issues. On the other hand, the WI units are getting more of interest for power generation rather than heat supply because not only electricity is more valued than heat in the energy market but also electricity driven

facilities, such as heat pumps and electrical boilers, are becoming more popular for district heating applications every day.

Comparing the results presented for the three different scenarios and the facts presented about the solar power plants and WI technologies, one may simply conclude that the proposed system is a smart solution to pave the bed for a reliable increase of the share of solar energy in the energy matrices and also provide the bed for bringing the WI units more into the electricity supply chains rather than district heating systems.

5. Conclusion

This study proposes a hybrid solar-waste driven Rankine power plant and presents a thorough thermodynamic modeling of the power plant for a case study in Denmark. The proposed design of the power plant makes the intermittent solar energy production dispatchable in a cost- and energy-efficient way. For the solar part of the combined plant, tracking PTCs are used to make the system capital cost lower and to make the use of a secondary balancing heat source rational. The choice of WI, as the secondary heat source of the plant, is due to the importance of this technology in European, especially Danish, energy matrix. The results of the simulations and assessments show that the use of a WI unit along with a PTC array for a steam power plant is a smart measure to increase the share of renewable energy with no need to any energy storage unit. In this way, the contribution of the WI technology in the future energy system could also increase as the best solution for waste disposal.

Overall, an acceptable annual energy efficiency of 24% is expected from the hybrid system which is 10% higher than a CSP plant with PTCs. In addition, the power sales profile of the CSP plant can be significantly improved when integrated with a WI unit. Although a solar power plant is considered 100% environmentally friendly, a hybrid CSP-WI system also can be considered as a highly sustainable system where a 10 MWe power plant in this configuration may prevent up to 8,000 tonnes of CO_2e per month compared to a gas power plant in the case study of this project.

Along with the many advantages of the proposed hybrid power plant, there are two main drawbacks for this study and the hybrid system. The first drawback is the fact that this system is only appropriate for the locations with efficient waste management service. The truth is that not all countries have such waste management facilities and this limits the appropriateness of the proposed system to the countries with waste incineration units as active elements of their energy systems. A further deficiency of this study is that it does not consider the part load and off-design operation of the system components; rather it presents a pseudo-dynamic modelling of the hybrid power plant. In addition, the existence of an optimized power sales strategy for the power plant can give a better picture of the realistic fluctuations of the loads and the

system dynamics. This, however, needs a very detailed information about the characteristics of each of the components of the system, their performance profiles, etc. Therefore, the future work of the authors in this context will be a fully dynamic modeling of the proposed hybrid power plant in a wide range of configurations as well as optimal sizing and the determination of an optimal power sales strategy for the plant.

References

[1] A.P. Roskilly, M. Ahmad Al-Nimr, Sustainable Thermal Energy Management, Energy Convers. Manag. 159 (2018) 396–397. doi:https://doi.org/10.1016/j.enconman.2017.12.018.

[2] A. Arabkoohsar, G.B. Andresen, A smart combination of a solar assisted absorption chiller and a power productive gas expansion unit for cogeneration of power and cooling, Renew. Energy. 115 (2018). doi:10.1016/j.renene.2017.08.069.

[3] A. Upadhyay, A. Chowdhury, Solar Energy Fundamentals and Challenges in Indian restructured power sector, Int. J. Sci. Res. Publ. 4 (2014) 2250–3153. www.ijsrp.org.

[4] E. Kabir, P. Kumar, S. Kumar, A.A. Adelodun, K.-H. Kim, Solar energy: Potential and future prospects, Renew. Sustain. Energy Rev. 82 (2018) 894–900. doi:https://doi.org/10.1016/j.rser.2017.09.094.

[5] J.J.C.S. Santos, J.C.E. Palacio, A.M.M. Reyes, M. Carvalho, A.J.R. Freire, M.A. Barone, Chapter 12 - Concentrating Solar Power, in: I.B.T.-A. in R.E. and P.T. Yahyaoui (Ed.), Elsevier, 2018: pp. 373–402. doi:https://doi.org/10.1016/B978-0-12-812959-3.00012-5.

[6] S.J. Smith, 14 - The long-term market potential of concentrating solar power (CSP) systems, in: K. Lovegrove, W.B.T.-C.S.P.T. Stein (Eds.), Woodhead Publ. Ser. Energy, Woodhead Publishing, 2012: pp. 437-e3. doi:https://doi.org/10.1533/9780857096173.2.437.

[7] B. Belgasim, Y. Aldali, M.J.R. Abdunnabi, G. Hashem, K. Hossin, The potential of concentrating solar power (CSP) for electricity generation in Libya, Renew. Sustain. Energy Rev. 90 (2018) 1–15. doi:https://doi.org/10.1016/j.rser.2018.03.045.

[8] M. Balghouthi, S.E. Trabelsi, M. Ben Amara, A.B.H. Ali, A. Guizani, Potential of concentrating solar power (CSP) technology in Tunisia and the possibility of interconnection with Europe, Renew. Sustain. Energy Rev. 56 (2016) 1227–1248. doi:https://doi.org/10.1016/j.rser.2015.12.052.

[9] O. Ogunmodimu, E.C. Okoroigwe, Concentrating solar power technologies for solar thermal grid electricity in Nigeria: A review, Renew. Sustain. Energy Rev. 90 (2018) 104–119. doi:https://doi.org/10.1016/j.rser.2018.03.029.

[10] A. Arabkoohsar, K.A.R. Ismail, L. Machado, R.N.N. Koury, Energy consumption minimization in an innovative hybrid power production station by employing PV and evacuated tube collector solar thermal systems, Renew. Energy. 93 (2016). doi:10.1016/j.renene.2016.03.003.

[11] Q. Mao, Recent developments in geometrical configurations of thermal energy storage for concentrating solar power plant, Renew. Sustain. Energy Rev. 59 (2016) 320–327. doi:https://doi.org/10.1016/j.rser.2015.12.355.

[12] C. Prieto, P. Cooper, A.I. Fernández, L.F. Cabeza, Review of technology: Thermochemical energy storage for concentrated solar power plants, Renew. Sustain. Energy Rev. 60 (2016) 909–929. doi:https://doi.org/10.1016/j.rser.2015.12.364.

[13] J.D. McTigue, J. Castro, G. Mungas, N. Kramer, J. King, C. Turchi, G. Zhu, Hybridizing a geothermal power plant with concentrating solar power and thermal storage to increase power generation and dispatchability, Appl. Energy. 228 (2018) 1837–1852. doi:https://doi.org/10.1016/j.apenergy.2018.07.064.

[14] F. Cavallaro, E.K. Zavadskas, D. Streimikiene, Concentrated solar power (CSP) hybridized systems. Ranking based on an intuitionistic fuzzy multi-criteria algorithm, J. Clean. Prod. 179 (2018) 407–416. doi:https://doi.org/10.1016/j.jclepro.2017.12.269.

[15] H.G. Jin, H. Hong, 12 - Hybridization of concentrating solar power (CSP) with fossil fuel power plants, in: K. Lovegrove, W.B.T.-C.S.P.T. Stein (Eds.), Woodhead Publ. Ser. Energy, Woodhead Publishing, 2012: pp. 395–420. doi:https://doi.org/10.1533/9780857096173.2.395.

[16] O. Behar, Solar thermal power plants – A review of configurations and performance comparison, Renew. Sustain. Energy Rev. 92 (2018) 608–627. doi:https://doi.org/10.1016/j.rser.2018.04.102.

[17] G. Manente, S. Rech, A. Lazzaretto, Optimum choice and placement of concentrating solar power technologies in integrated solar combined cycle systems, Renew. Energy. 96 (2016) 172–189. doi:https://doi.org/10.1016/j.renene.2016.04.066.

[18] European Waste Incineration Directive, (2007). http://ec.europa.eu/environment/archives/air/stationary/wid/legislation.htm.

[19] W. Yang, H.-S. Nam, S. Choi, Improvement of operating conditions in waste incinerators using engineering tools, 2007. doi:10.1016/j.wasman.2006.04.016.

[20] European Commission, The role of waste-to-energy in the circular economy, Commun. From Comm. To Eur. Parliam. Counc. Eur. Econ. Soc. Comm. Comm. Reg. (2017) 11. http://ec.europa.eu/environment/waste/waste-to-energy.pdf.

[21] Z. Ghouleh, Y. Shao, Turning municipal solid waste incineration into a cleaner cement production, J. Clean. Prod. 195 (2018) 268–279. doi:https://doi.org/10.1016/j.jclepro.2018.05.209.

[22] M. Münster, P. Meibom, Optimization of use of waste in the future energy system, Energy. 36 (2011) 1612–1622. doi:https://doi.org/10.1016/j.energy.2010.12.070.

[23] O. Eriksson, G. Finnveden, T. Ekvall, A. Björklund, Life cycle assessment of fuels for district heating: A comparison of waste incineration, biomass- and natural gas combustion, Energy Policy. 35 (2007) 1346–1362. doi:https://doi.org/10.1016/j.enpol.2006.04.005.

[24] N.A. and S. Administration, A Hybrid Pyrolysis/Incineration System for Solid Waste Resource Recovery, 2003. https://www.sbir.gov/sbirsearch/detail/75099.

[25] K. Udono, R. Sitte, Modeling seawater desalination powered by waste incineration using a dynamic systems approach, Desalination. 229 (2008) 302–317. doi:https://doi.org/10.1016/j.desal.2007.10.017.

[26] E. Hedberg, D. Project, Potential for Absorption Cooling Generated from Municipal Solid Waste in Bangkok, (n.d.).

[27] A. Arabkoohsar, G.B. Andresen, Thermodynamics and economic performance comparison of three high-temperature hot rock cavern based energy storage concepts, Energy. 132 (2017). doi:10.1016/j.energy.2017.05.071.

[28] J.P. Stark, Fundamentals of classical thermodynamics (Van Wylen, Gordon J.; Sonntag, Richard E.), J. Chem. Educ. 43 (1966) A472. doi:10.1021/ed043pA472.1.

[29] V.E. Dudley, G.J. Kolb, A.R. Mahoney, T.R. Mancini, C.W. Matthews, M. Sloan, D. Kearney, Dudley V; Kolb G; Sloan M; Kearney D., Test results: SEGS LS-2 solar collector, Sandia Natl. Lab. (1994).

[30] R. Dickes, V. Lemort, S. Quoilin, Semi-empirical correlation to model heat losses along solar parabolic trough collectors, 2015.

[31] A. Valan Arasu, T. Sornakumar, Design, manufacture and testing of fiberglass reinforced parabola trough for parabolic trough solar collectors, Sol. Energy. 81 (2007) 1273–1279. doi:https://doi.org/10.1016/j.solener.2007.01.005.

[32] E.M.A. Mokheimer, Y.N. Dabwan, M.A. Habib, S.A.M. Said, F.A. Al-Sulaiman, Techno-economic performance analysis of parabolic trough collector in Dhahran, Saudi Arabia, Energy Convers. Manag. 86 (2014) 622–633. doi:https://doi.org/10.1016/j.enconman.2014.06.023.

[33] A. Arabkoohsar, L. Machado, M. Farzaneh-Gord, R.N.N. Koury, Thermo-economic analysis and sizing of a PV plant equipped with a compressed air energy storage system, Renew. Energy. 83 (2015). doi:10.1016/j.renene.2015.05.005.

[34] V. Gnielinski, New equations for heat and mass transfer in turbulent pipe and channel flow., Int. Chem. Eng. 16 (1976) 359–368.

[35] F.P. Incropera, T.L. Bergman, A.S. Lavine, D.P. DeWitt, Fundamentals of Heat and Mass Transfer, 2011. doi:10.1073/pnas.0703993104.

[36] Y.S. Touloukian and D.P. DeWitt, hermal radiative properties, Nonmetalic Solids. (1972).

[37] A. Arabkoohsar, G.B. Andresen, Supporting district heating and cooling networks with a bifunctional solar assisted absorption chiller, Energy Convers. Manag. 148 (2017) 184–196. doi:https://doi.org/10.1016/j.enconman.2017.06.004.

[38] US Environmental Protection Agency (USEPA), (n.d.). https://www.epa.gov/.

[39] M.K. Johnke B, Hoppaus R, Lee E, Irving B, Martinsen T, Good practice guidance and uncertainty management in national greenhouse gas inventories., 2000.

[40] Historical Solar Irradiation Data in Denmark, (n.d.). http://irradiance.dmi.dk/irradiance-data/.

[41] A. Arabkoohsar, K.A.R. Ismail, L. Machado, R.N.N. Koury, Energy consumption minimization in an innovative hybrid power production station by employing PV and evacuated tube collector solar thermal systems, Renew. Energy. 93 (2016) 424–441. doi:https://doi.org/10.1016/j.renene.2016.03.003.

[42] B. Zhao, M. Cheng, C. Liu, Z. Dai, System-level performance optimization of molten-salt packed-bed thermal energy storage for concentrating solar power, Appl. Energy. 226 (2018) 225–239. doi:https://doi.org/10.1016/j.apenergy.2018.05.081.

[43] M. Farzaneh-Gord, A. Arabkoohsar, M.D.D. Bayaz, A.B. Khoshnevis, New method of solar energy application in greenhouses to decrease fuel consumption, Int. J. Agric. Biol. Eng. 6 (2013). doi:10.3965/j.ijabe.20130604.008.

[44] K. Dong, R. Sun, X. Dong, CO2 emissions, natural gas and renewables, economic growth: Assessing the evidence from China, Sci. Total Environ. 640–641 (2018) 293–302.

doi:https://doi.org/10.1016/j.scitotenv.2018.05.322.

Nomenclature

Sign	Parameter	Unit
A	Area	m^2
D	Diameter	m
E_{CO2e}	Amount of CO_2e emission	-
$\dot{E}_{gen}$	Electricity power	kW
E_λ	Emission of different types of greenhouse gases	-
f	Friction factor for a pipe surface	-
GWP_λ	Global warming potential of greenhouse gases	-
h	Enthalpy	kJ/kg
h_c	Convective heat transfer coefficient	kJ/m2.K
Δh_{PTC}	Enthalpy change of the working fluid of the solar system	kJ/kg
Δh_{WI}	Enthalpy change of WI working fluid	kJ/kg
IAM	Incidence angle modifier	-
K	Thermal conductance	kJ/m.K
LHV	Low heat value	kJ/kg
M	Mass of the waste	kg
Nu	Nusselt number	-
Pr	Prandtl number	-
q'_{12conv}	Convective heat transfer between solar working fluid and the absorber	kJ/m
q'_{23cond}	Conductive heat transfer through the absorber wall	kJ/m
q'_{34rad}	Heat transfer from the absorber to the glass envelope	kJ/m
$q'_{3SolAbs}$	Solar heat absorbed by the absorber	kJ/m
q'_{45cond}	Conductive heat transfer through the glass envelope	kJ/m
q'_{56conv}	Convective heat transfer from the glass envelope to the atmosphere	kJ/m
q'_{56rad}	Radiative heat transfer from the glass envelope to the atmosphere	kJ/m
q'_{57rad}	Radiative heat transfer from the glass envelope to the sky	kJ/m
$q'_{5SolAbs}$	Solar absorption in the glass envelope	kJ/m
q'_{cond}	Heat rejected in Condenser	kJ/m
$q'_{cond,bracket}$	Conductive heat transfer through the bracket support	kJ/m
q'_{si}	Solar irradiation per receiver length	kJ/m
$\dot{Q}_{cond}$	Rate of heat rejected in condenser	kW
$\dot{Q}_{WI}$	Heat released in waste incineration process	kW
Re	Reynolds number	-
$\dot{m}_{ph1}$	Mass flow rate of the first preheating line	kg/s
$\dot{m}_{ph2}$	Mass flow rate of the Second preheating line	kg/s
$\dot{m}_{PTC}$	Mass flow rate solar field	kg/s
$\dot{m}_{st}$	Total mass flow rate of steam	kg/s

$\dot{m}_{WI}$	Mass flow rate waste incineration plant	kg/s
r_{conc}	Concentrator reflectance	-
T	Temperature	K
w	Specific work	kJ/kg
$\dot{W}$	Work production rate	kW

Greek symbols

α_{abs}	Absorptance of the absorber
α_{env}	Absorptance of the envelope
ε	Emittance
ε_1'	Shadowing factor
ε_2'	Tracking error
ε_3'	Geometry error (mirror alignment)
ε_4'	Dirt on mirrors
ε_5'	Dirt on collector
ε_6'	Unaccounted factor
η_{abs}	Effective optical efficiency at absorber
η_{env}	Effective optical efficiency at the glass envelope
η_{gen}	Electricity generation efficiency
ξ	Exhaust gas volume
η_{WI}	Thermal efficiency of waste incineration plant
ρ_{cl}	Clean mirror reflectance
τ	Transmittance
τ_{env}	Transmittance of the envelope

Subscripts

abs	Absorber
blr	Boiler
c	Cover
ci	Cover inner
co	Cover outer
conc	Concentrator
cond	conduction
conv	Convection
env	Envelope
gen	Generation
hpt	High pressure turbine
ipt	Intermittent pressure turbine
lpt	Low pressure turbine
ng	Natural gas
P	Pump
r	receiver
rad	Radiation
ri	Receiver inner
ro	Receiver outer
Sol	Solar
WI	Waste incineration

wst	waste

- A hybrid concentrating solar power plant accompanied with a waste incineration unit is proposed.
- The proposed system provides a cost-effective and dispatchable electricity to the grid.
- Thermodynamic performance and environmental impacts of the system are investigated.
- The net annual energy efficiency of the system is approximately 24%.
- The system contributes to the prevention of a large amount of CO_2e emission.